1-25-2019 1:00 PM

Investigating the Role of Tp53INP1 and Tp53INP2 in Neuronal Autophagy and Mitophagy

Vidhyasree Shyam, *The University of Western Ontario*

Supervisor: Cregan, Sean, *The University of Western Ontario*
A thesis submitted in partial fulfillment of the requirements for the Master of Science degree in Neuroscience

Recommended Citation

Abstract

Autophagy is highly conserved cellular process that function in ensuring the turnover of proteins and organelles in a number of different cell types. Mitophagy is a selective form of autophagy which serves to target and rid the cell of damaged or superfluous mitochondria. The process is central to preventing the accumulation of defective mitochondria and is particularly important in neurons, which rely exclusively on mitochondria to sustain their immense metabolic needs. Dysregulation of autophagy is believed to contribute to the neurodegeneration seen in such disorders as Parkinson's disease and cerebral ischemia. However, further understanding of the role of neuronal autophagy under stress conditions, and the relevant players involved in this process is required. In recent years, two homologous proteins expressed only in higher eukaryotes have been described to play roles in mammalian autophagy and mitophagy. Tumour- protein 53-induced nuclear protein 2 (Tp53INP2) has a bi-functional role as a modulator of autophagy and gene transcription. This protein was shown to participate in non-neuronal autophagy, however its role in mitophagy is not well understood. Additionally, tumour- protein 53-induced nuclear protein 1 (Tp53INP1), has been suggested to play a role in autophagy as well as PINK1/Parkin mitophagy, however neither protein has been investigated in neuronal paradigms. Our findings demonstrate that cerebellar granule neurons and primary cortical neurons from Tp53INP1$^{-/-}$ mice demonstrate attenuated autophagy induction in response to trophic factor deprivation and hypoxic stress, respectively. We also demonstrate through confocal microscopy that Tp53INP2 responds to CCCP-induced mitochondrial stress by shuttling out of the nucleus and co-localizing with autophagosomal protein LC3, suggesting that it may play a role in mitophagy.

Keywords:

Tp53INP1, Tp53INP2, Autophagy, Mitophagy, Hypoxia, Mitochondrial stress, LC3

Acknowledgments

First and foremost, I would like to give my greatest thanks to my supervisor Dr. Sean Cregan, without whom I could not have begun nor completed this journey. Thank you for providing me with the opportunity to begin this my master's under your supervision, as well as endless support and guidance even until the very end. You are an outstanding scientist and a truly incredible human being, and it was an honour working with you. I would also like to thank the members of my advisory committee for, Dr. Stephen Pasternak and Dr. Martin Duennwald, for sharing their knowledge and expertise and providing me guidance throughout the course of my thesis.

A sincere thank you to all the incredible individuals that I had the pleasure of meeting throughout my Masters. In particular my greatest thanks to all the members of the Cregan Lab both past and present, who collectively created a collaborative and enjoyable work environment, and of whom I have made some of my fondest memories with. A special thank you to our lab technician, Heather-Tarnowski-Garner for supporting my project in numerous ways and always lending a helping hand when needed.

A whole-hearted thank you to my colleague and best friend Fatemeh Mirshafiei Langari. Thank you for not only providing me with endless emotional support, but for brightening every day of my journey. You are a fighter; your persistence and resilience does not go unseen, and I have no doubt that you will make an incredible scientist one day. But most of all you are kind and full of light, and to have met such an incredible soul was truly a blessing. The world needs more people like you.

Thank you to Dr. Asit Rai, whose scientific expertise helped me to overcome many obstacles in my project and whose advice I will hold on to well into my future. Your kindness throughout my masters will not be forgotten, and I am incredibly grateful to call you a friend.

Last but not least, to my parents, Mohan and Priya, and my siblings Vivek and Vinaya, thank you for believing in me more than I believe in myself. For instilling in me the value of hard work and demonstrating to me that there is no adversity we cannot overcome together. Thank you for always providing me with unconditional love and support, you are truly my greatest blessing.

Table of Contents

List of Tables

List of Figures

List of Appendices

List of Abbreviations

Aβ	Amyloid beta
AD	Alzheimer's disease
Akt	Protein kinase B
AMPK	5' adenosine monophosphate-activated protein kinase
APP	Amyloid precursor protein
ATG5	Autophagy related protein 5
ATG12	Autophagy related protein 12
ATG13	Autophagy related protein 13
ATG16	Autophagy related protein 16
ATP	Adenosine triphosphate
AV	Autophagic vacuoles
Baf A1	Bafilomycin A1
BCA	Bicinchoninic acid assay
BNIP3	BCL2-interacting protein 3
BSA	Bovine serum albumin
CCCP	Carbonyl cyanide m-chlorophenyl hydrazone
CGNs	Cerebellar granule neurons
CMA	Chaperone -mediated autophagy
CNS	Central nervous system
CO_2	Carbon dioxide
CPT	Camptothecin
CQ	Chloroquine
CRSIPR/Cas 9	Clustered regularly interspersed short palindromic repeats

CTRL	Control
DFCP1	EEA1 domain-containing protein 1
DJ-1	Protein/nucleic acid deglycase
DMEM	Dulbecco's modified eagle medium
DNA	Deoxyribonucleic acid
DOR	Diabetes and obesity-regulate gene
Drp1	Dynamin-related protein 1
eGFP	Enhanced green fluorescent protein
E14	Embryonic day 14
FBS	Fetal bovine serum
FIP200	FAK family-interacting protein of 200 kDa
GABARAP	Gamma-aminobutyric acid receptor-associated protein
GABARAPL1	Gamma-aminobutyric acid receptor-associated protein-like1
GBA	β-glucocerebrosidase
GDP	Guanosine-5'-diphosphate
GTP	Guanosine-5'-triphosphate
HBSS	Hank's Balanced Salt Solution
HD	Huntington's disease
HeLa	Human cervical cancer cell line
HIPK2	Homeodomain-interaction protein kinase 2
HIF-1α	Hypoxia-inducible factor 1α
H/I	Hypoxia/ischemia
HRP	Horseradish peroxidase
Hsc70	Heat shock cognate protein 70kDa
Htt	Huntingtin gene

K5	5mM KCl
K25	5mM KCl
KCl	Potassium chloride
KFERQ	Lysine, phenylalanine, glutamic acid, arginine, glutamine
KO	Knockout
LAMP2	Lysosomal associated membrane protein 2
LC3	Microtubule-associated protein light chain 3
LIR	LC3-interacting region
LRRK2	Leucine rich repeat kinase 2
3-MA	3-methyladenine
MDC	Monodansylcadaverine
mCherry	Red fluorescent protein
MEFs	Mouse embryonic fibroblasts
MEM	Minimal essential media
Mfn2	Mitofuscin 2
MOMP	Mitochondrial outer membrane permeabilization
MPP	Mitochondrial processing peptidase
mRNA	Messenger ribonucleic acid
mTOR	Mammalian target of rapamycin kinase
NBR1	Neighbor of BRCA1 gene 1 protein
ND	Neurodegenerative disease
NES	Nuclear export signal
OGD	Oxygen-glucose deprivation
p53	Tumour protein 53
p62/SQSTM1	Sequestosome-1

PARL	Presenilin-associated rhomboid-like protein
PBS	Phosphate buffered saline
PCN	Primary cortical neurons
PCR	Polymerase chain reaction
PD	Parkinson's disease
PE	Phosphatidylethanolamine
PI3P	Phosphatidylinositol 3- phosphate
PI3K	Phosphoinositide 3-kinase
PINK1	PTEN-induced putative kinase 1
PKCδ	Protein kinase C delta
PML-NBs	Promyelocytic leukaemia protein- nuclear bodies
Poly-Q	Poly glutamine
Pro-LC3	Unprocessed LC3
Rheb	Ras homolog enriched in brain
RIPA	Radioimmunoprecipitation assay
ROS	Reactive oxygen species
RNA	Ribonucleic acid
RP	Reperfusion
RT-PCR	Reverse transcription polymerase chain reaction
SEM	Standard error of the mean
SIP	Stress inducible protein
TOM	Translocase of the outer mitochondrial membrane
TIM	Translocase of the inner mitochondrial membrane
Tp53INP1/2	Tumour protein 53 induced nuclear protein 1 and 2
TSC1-TSC2	Tuberous sclerosis complex 1 and 2

U2OS	Human bone osteosarcoma cell line
ULK1/2	Unc-51-like kinase 1/2
UPS	Ubiquitin-proteasome system
UT	Untransfected
VPS34	Vacuolar protein sorting 34
WIPW	WD-repeat protein interacting with phosphoinositides
WT	Wildtype

Chapter 1

1   Introduction

1.1   Autophagy

Autophagy is an intracellular response involving the sequestration and subsequent degradation of old, damaged or superfluous macromolecules and organelles at the lysosome. This catabolic process is most notably induced under starvation conditions characterized by a deficiency in glucose or amino acids and an increase in AMP-activated protein kinase (AMPK). In addition to this, autophagy functions to clear the cell of damaged proteins and organelles and has conserved roles in cell differentiation and development (Mizushima & Levine , 2010).

The process can take place through three major forms including chaperone-mediated autophagy (CMA) in which soluble unfolded proteins with the KFERQ motif are recognized and transported to the lysosome by heat shock cognate protein 70kDa (hsc70), microautophagy in which small cytosolic volumes are directly engulfed through invagination of the lysosomal membrane, as well as macroautophagy involving expansion of an isolation membrane around the contents of interest into a double membraned vesicle, and its subsequent degradation via fusion with the lysosome (Figure 1.1) (Nedelsky, Todd & Taylor, 2008). Among these, macroautophagy (hereafter referred to as autophagy) has been the most extensively studied. Under basal conditions the process serves to continuously recycle intracellular pools of macromolecules and organelles, playing a critical role in maintaining cellular homeostasis. Following internal or external stressors, the process is upregulated thereby exerting key cytoprotective roles. Autophagy was initially believed to work non-selectively in response to starvation, resulting in bulk degradation of cytosolic contents. However, studies have demonstrated the ability of the process to selectively target specific molecules dependent on the stress induced, although how this selectivity is initiated is still not well understood. Examples of selective autophagy that have been observed include mitochondria (mitophagy), ribosomes (ribophagy), peroxisomes (pexophagy), aggregate proteins (aggrephagy) and foreign invaders

(xenophagy) (Stolz, Ernst & Dikic, 2014). This selectivity is largely carried out by autophagy receptors which are able to recognize and bridge cargo as well as autophagosomal membrane protein microtubule-associated protein light chain 3 (LC3). Since one of the most prevalent and recognized autophagy signals involves ubiquitin modifications, most of these receptors also retain a ubiquitin binding domain, in addition to their LC3-interacting region (LIR). An example of these includes p62/SQSTM1 (sequestosome-1) and neighbor of BRCA1 gene 1 protein (NBR1) (Stolz, Ernst & Dikic, 2014).

1.2   Molecular Mechanisms of Autophagy

Autophagy induction is regulated primarily by mammalian target of rapamycin (mTOR) kinase which acts to prevent autophagy from initiating during nutrient abundant conditions by blocking Unc-51-like kinase (ULK)1/2 complex, an initial inducer of autophagy. However, during starvation conditions, mTOR is inhibited by 5' adenosine monophosphate-activated protein kinase (AMPK), as well as tuberous sclerosis complex 1 and 2 (TSC1-TSC2), thereby causing the activation of ULK1/2 complex. Autophagosome biogenesis begins with the proteins of the ULK1/2 complex assembling. Nucleation of the autophagosome requires the activated ULK1/2 complex to autophosphorylate and phosphorylate autophagy related protein 13 (ATG13) and FAK family-interacting protein of 200 kDa (FIP200), two proteins in the ULK1/2 complex (Figure 1.2). The activated complex then phosphorylates Beclin1 thereby activating the Beclin1-vacuolar protein sorting 34 (VSP34) complex which acts as a class III phosphoinositide 3-kinase (PI3K). The complex produces phosphatidylinositol 3-phosphate (PI3P) which recruits WD-repeat protein interacting with phosphoinositides (WIPI) and EEA1 domain-containing protein 1 (DFCP1) which play roles in generating the isolation membrane (phagophore) that serves as the premature membrane of the autophagosome (Kiriyama & Nochi, 2015).

Next, a complex composed of ATG12, ATG5 and ATG16 is recruited to the autophagosomal membrane to facilitate the lipidation of LC3, a protein necessary for the expansion of the isolation membrane with a phosphatidylethanolamine (PE) lipid tail. LC3, is associated directly with the autophagsome and remains associated until the process is complete. Unprocessed pro-LC3 is co-translationally cleaved into its cytosolic form LC3-

I. Upon autophagy stimulus, LC3-I becomes conjugated to a PE lipid tail to form LC3-II, which can now covalently bind directly to the autophagosomal membrane and contribute to the elongation of the isolation membrane into the autophagosome (Tanida, Ueno, & Kominami, 2004). This direct association between LC3-II and the autophagosome allows it to serve as a reliable marker of autophagsomes for immunofluorescence and immunoblotting studies (Figure 1.3). Additionally, the generation and turnover of LC3-II is used as an accurate indication of autophagy flux, as the increase in conversion of LC3-I to LC3-II indicates an increase in autophagosome formation and therefore an increase in autophagy (Nedelsky, Todd, & Taylor , 2008). Since autophagy is a dynamic process, the use of lysosomal inhibitors such as chloroquine (CQ) and bafilomycin A1 (baf A1) can further capture the change in autophagic flux by preventing autophagosome turnover and thereby LC3-II turnover.

Upon enclosure of the double membraned autophagosome around the cargo, the autophagosome fuses with the lysosome to form the autolysosome. This fusion allows for lysosomal acid hydrolases to degrade the inner autophagosomal membrane as well as the cargo within. The degradation products are then released back to the cytosol to be recycled by the cell.
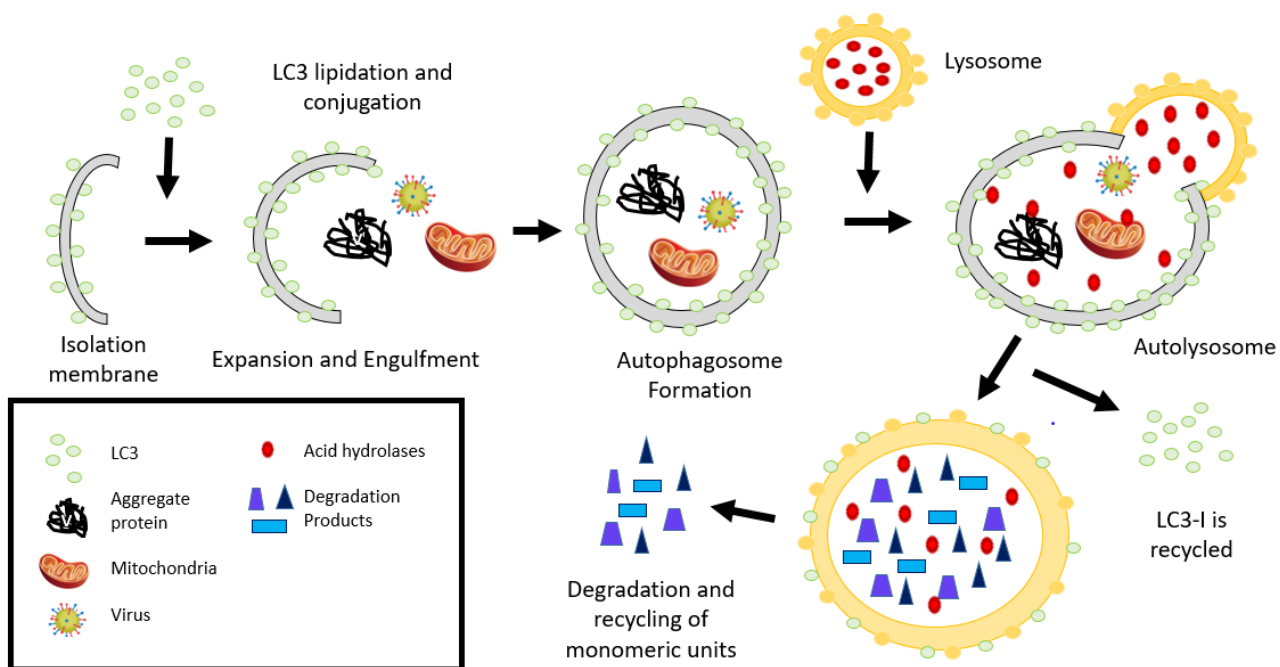
Figure 1.1 The Mechanism of Mammalian Autophagy: In mammalian autophagy, initiation begins with the expansion of the isolation membrane by several autophagy-related proteins including LC3 around the cellular contents to be removed. The autophagosome is formed upon closure of the double-membraned organelle. Fusion of the lysosome with the autophagosome results in a hybrid autolysosome, in which lysosomal acid hydrolases degrade autophagosomal contents and inner autophagosomal membrane. The degraded products are then expelled to the cytosol for cellular use.
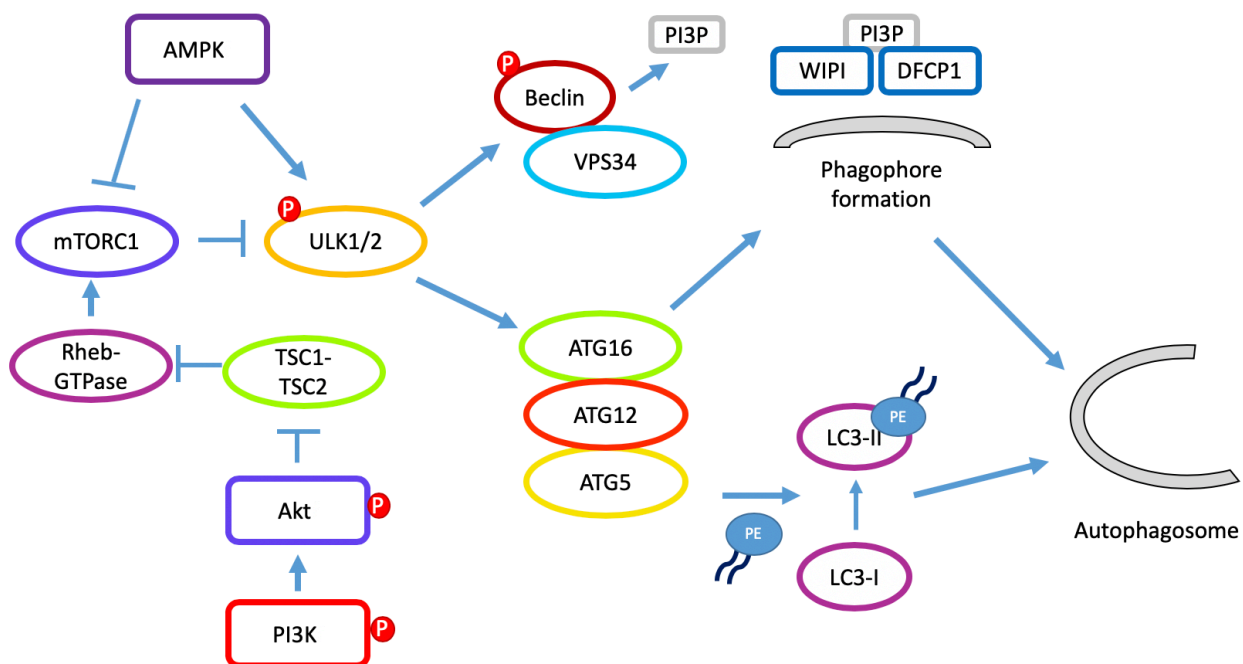
Figure 1.2 The signaling pathway of mammalian autophagy: Autophagy is primarily regulated by activated mTOR, a nutrient sensing kinase that serves to prevent autophagy induction during nutrient abundant conditions. However, as AMP concentrations rise, 5' adenosine monophosphate-activated protein kinase (AMPK) inactivates mTOR to promote autophagy by allowing the autophosphorylation and activation of Unc-51-like kinase 1/2 (ULK1/2), therefore allowing it to activate the Beclin1-VPS34 complex. This complex functions as a class III phosphoinositide 3-kinase (PI3K) producing phosphatidylinositol 3-phosphate (PI3P) which serves to recruit WIPI and DFCP1. WIPI and DFCP1 are PI3P binding proteins that aid in formation of the phagophore membrane. ULK1/2 also interacts with ATG16- ATG5-ATG12, a complex that functions to conjugate phosphatidylethanolamine (PE) to LC3-I to form the activated LC3-II that contributes to the formation and elongation of the autophagosomal membrane. Additionally, mTOR inactivation can negatively regulated by tuberous sclerosis complex 1 and 2 (TSC1-TSC2) complex, by stimulating the conversion of Ras homolog enriched in brain (Rheb)-GTP to Rheb-GDP. Under anabolic conditions TSC1-TSC2 complex is inhibited by the phosphoinositide 3-kinase (PI3K)/ protein kinase B (Akt) pathway.
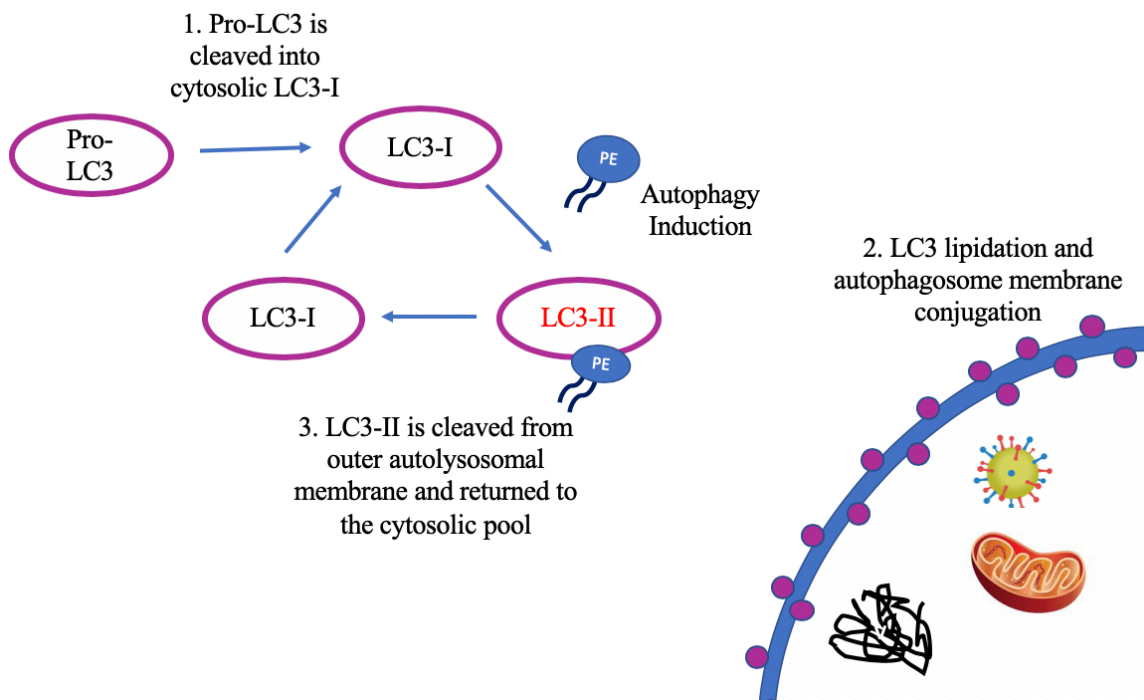
Figure 1.3. Processing of LC3 upon autophagy induction. Unprocessed Microtubule-associated protein 1 light chain 3 (Pro-LC3) is synthesized is cleaved of is amino acids from the C-terminus side to produce LC3-I.   LC3-I becomes conjugated to phosphatidylethanolamine tail upon autophagy induction converting it to LC3-II. LC3-II is incorporated into the autophagosomal membrane to contribute the elongation of the autophagosome. LC3-II is the only marker that is reliably associated with completed autophagosomes. Upon autophagy completion, LC3-II bound to the inner autophagosomal membrane becomes degraded, and that on the outer autophagosomal membrane is cleaved and converted back into LC3-I.

1.3 Neuronal Autophagy

The demand for basal autophagy can often vary depending on the tissue, being particularly important in the liver and in cells that do not divide after differentiation such as myocytes and neurons. It was generally believed that basal autophagy in neurons occurred at low levels due to the neuronal ability to not only use glucose, but ketones as an alternative source of energy. Additionally, neighboring astrocytes can provide short term energy stores through the conversion of glucose into lactate (Gabryel, Kost and Kasprowska, 2012). Basal autophagy is thought to be a protective process in neurons, playing important roles in synaptic plasticity, anti-inflammatory roles of glial cells and myelination of oligodendrocytes (Nah, Yuan, & Jong, 2015). The process is constitutive in neurons, acting non-selectively under nutrient deprived conditions. It plays a crucial role in the homeostasis of neurons, and the removal of aggregate prone proteins specifically, as neurons cannot dilute their cellular burdens through cell division. In particular, because neurons retain highly specialized structures that rely heavily on adequate intracellular communication and transport of material across large axonal distances, well-regulated quality control mechanisms such as autophagy must exist.

Additionally, previous studies have used knockout models to demonstrate the importance of autophagy in various cell types including neurons. Unlike conventional *atg5* and *beclin1* knockout mice which do not survive past embryogenesis, neural-tissue-specific knockouts which survive past the postnatal starvation period, display progressive motor deficits. Specifically, Komatsu et al., demonstrated that complete impairment of autophagy in the central nervous system resulted in marked reductions in large pyramidal cells and Purkinje cells in the cortical and cerebral cortices, respectively (Komatsu, et al., 2006). Additionally an age dependent increase in the number and size of ubiquitin positive inclusion bodies, known pathological hallmarks of various neurodegenerative diseases (NDs) were also observed (Komatsu et al., 2006). Therefore, it is evident that basal levels of autophagy are imperative to the functioning and survival of neurons and that impairment of these processes can lead to the accumulation of aberrant proteins.

1.4   Autophagy and Neurodegeneration

Many types of neurodegenerative diseases are accompanied by the accumulation of aggregate ubiquitinated proteins as well as an accumulation of autophagosomes. The former indicative of inadequate proteosomal or lysosomal degradation processes, and the latter indicating an imbalance between autophagosome formation and autophagosome degradation. In particular, this fundamental balance between too little or too much autophagy is believed to contribute to its dual role as being cytoprotective and a contributor of cell death (Figure 1.4).
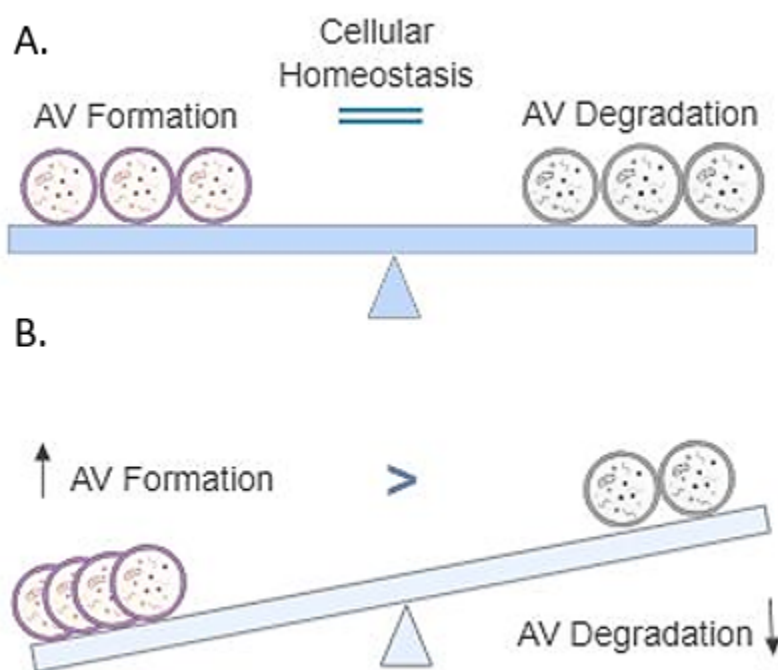
Figure 1.4 The balance in autophagic flux in neurons is crucial to cellular homeostasis: The abnormal accumulation of autophagic vacuoles is common neuronal phenotype in neurodegenerative brains. *A.* The balance between autophagosome formation at basal levels or as a result of stress induction is balanced with autophagosome degradation at the lysosome, thereby maintain homeostasis. *B.* Under neurodegenerative states, either increased autophagosome formation or impaired degradation can lead to an increase in autophagic vacuoles deposition, and thereby autophagic stress.

1.4.1   Alzheimer's Disease

Alzheimer's disease (AD) is the most common form of senile dementia and has been characterized by the accumulation of amyloid beta (Aβ) plaques. Electron studies on AD brains provide evidence of alteration of autophagy in dystrophic neurons. These neurites retained abundant accumulation of autophagic vacuoles (AV), particular immature AVs suggesting impairment of late stage autophagy as well as retrograde transport to the lysosomes (Son, Shim, Kim, Ha & Han, 2012). Additionally, immunolabelling studies identified AVs to contain large amounts of Aβ, serving as a reservoir for both full length amyloid precursor protein (APP) and β-secretase cleaved APP. Furthermore, downregulation of *beclin1* has been observed in AD brains. The reduced expression of beclin1 in APP transgenic mice resulted in increased intraneuronal Aβ accumulation and extracellular Aβ deposition, as well as increased neurodegeneration (Nah, Yuan, & Jong, 2015).

1.4.2   Huntington's Disease

Huntington's disease (HD) is a movement disorder characterized by the loss of motor control and emergence of cognitive deficits. It is caused by expanded trinucleotide repeats (CAG) in the huntingtin (htt) gene that results in an abnormally long poly-glutamine (polyQ) expansion at the N-terminus of the protein. The polyQ expansion affects the structure of the protein and therefore its function, in addition to creating toxic aggregates that damage subcortical regions of the forebrain and the striatum. Htt plays an important role in autophagy by contributing to cargo recognition through its interaction with autophagosomal membrane-bound LC3 and p62-bound cargo (Rui, et al., 2015). However, alterations in autophagy have been observed in various models of HD, contributing to the insufficient clearance of mutant htt aggregates. Several reports have suggested that both mTOR-dependent and independent pathways enhance htt clearance and alleviate HD-associated behavioural and motor phenotypes (Rui et al., 2015).

1.4.3   Parkinson's Disease

Parkinson's disease (PD) is a progressive movement disorder that results in the loss of dopaminergic neurons in the substantia nigra. The disease is associated with the accumulation of cytosolic protein α-synuclein within inclusions called Lewy bodies, and

has displayed patterns of increased autophagosome-like structures. 90% of PD cases are sporadic, however familial mutations occur in specific genes including, α -synuclein (SNCA), Parkin (PARK2), PTEN-induced putative kinase 1 (PINK1) (PARK6), DJ-1(PARK7), B-glucocerbrosidase (GBA), and leucine-rich repeat kinase 2 (LRRK2). Accounting for the majority of autosomal recessive cases involve mutations in Parkin and PINK1, two proteins involved in mitophagy, the targeted removal of mitochondria by the autophagosome. Thus, these mutations abolish the cells ability to clear mitochondria, resulting in the accumulation of damaged mitochondria and the release of reactive oxygen species (ROS) as well as the potential initiation of apoptotic events (Nixon & Yang, 2012). Additionally, α -synuclein contains a KFERQ motif, and can thereby be degraded by both macroautophagy as well as CMA. However, mutations in the protein cause it to bind abnormally tightly to lysosomal associated membrane protein 2 (LAMP2) preventing its own uptake into the lysosome as well as uptake of other CMA substrates (Kiriyama & Nochi, 2015).

1.5   Mitophagy

Mitochondria are organelles central to cellular function and homeostasis. They provide an essential source of ATP necessary for cell survival as well as contribute to cellular stress responses such as autophagy and apoptosis. These complex organelles routinely undergo processes of fission and fusion that serve to modulate their form and function. Mitochondria are abundant in most cells and can occupy 10-40% of the cell volume (Hamacher-Brady & Brady, 2016). They can exist as a homogenous population or heterogeneously as seen in neuronal cell types. Appropriate mitochondrial functioning and quality control is particularly important in neurons. The central nervous system (CNS) while accounting for only 2% of the body's weight, consumes up to 20% of inspired oxygen at rest. This is due to the nervous system's vital dependence on oxidative phosphorylation to produce to immense amounts of ATP necessary for the highly specialized functions of neurons (Kann & Kovacs, 2006). In addition to ATP production, mitochondria function in establishing ion gradients for neurotransmission. Additionally, the unique morphology of neurons require mitochondrial trafficking through narrow axons to distant terminals, creating vulnerability to trafficking defects. This can be exasperated by their post-mitotic nature, debilitating them from preventing the build-up of damaged cell contents through

cellular division. Accumulation of damaged mitochondria via dysregulated mitophagy can result in increased release of ROS as well as the premature release of pro-apoptotic signals through mitochondrial outer membrane permeabilization (MOMP).

Mitophagy is a form of selective autophagy pathway that utilizes the cell's autophagic machinery to specifically remove mitochondria. The process occurs under physiological conditions, during the maturation of erythrocytes and the development of a fertilized oocyte, and as a form of quality control to maintain the balance between mitochondrial biogenesis and turnover (Kann & Kovacs, 2006). Mitophagy can also be induced in response to mitochondrial damaging conditions such as hypoxia, resulting in the removal of dysfunctional mitochondria. The process requires specific mitochondrial proteins to mark the mitochondria for recognition by the phagophore, followed by its subsequent degradation at the lysosome. In healthy mitochondria, oxidative phosphorylation is a key functional unit that generates ROS as a by-product. In dysfunctional mitochondria however, ROS levels become elevated and activate apoptosis (Jezek, Cooper, & Strich, 2018). When mitochondria become deficient, they undergo fission, becoming separated from the mitochondrial network. These mitochondria can then be separated into polarized and depolarized mitochondria, in which the latter is targeted for mitophagy. The process of fission is mediated by dynamin-related protein 1 (Drp1), a cytosolic protein that wraps around the mitochondria, severing the inner and outer membrane between two daughter cells forcing division that results in unequal polarization (Ashrafi and Schwarz, 2012).

1.5.1   PINK1/Parkin Mitophagy

One of the most studied pathways of mitophagy is known as PINK1/ Parkin mitophagy. PINK1 is a serine-threonine protein kinase that acts as a mitochondrial stress sensor, initiating mitophagy during mitochondrial membrane depolarization, misfolded mitochondrial protein and ROS generation (Song, Mihara, Chen, Scorrano & Dorn, 2015). Under basal conditions when mitochondria are healthy, PINK1 is targeted to the mitochondria and its accumulation on the outer mitochondrial membrane is prevented by its import through the outer mitochondrial membrane. Transport is facilitated by both outer mitochondrial membrane translocase (TOM) complex and inner mitochondrial membrane translocase (TIM) complex, where it is cleaved by mitochondrial proteases presenilin-

associated rhomboid-like protein (PARL) and mitochondrial processing peptidase (MPP). The cleaved kinase is then released into the cytosol, and degraded by the ubiquitin-proteasome system (UPS) (Martinez-Vincente, 2017). For this reason, mitochondrial levels of PINK1 are low in healthy mitochondria. Upon mitochondrial damage however, mitochondria lose their membrane potential preventing the complete processing of PINK1. Full-length PINK1 rapidly accumulate across the surface of the mitochondria with its kinase domain facing the cytosol. This allows it to phosphorylate ubiquitin substrates on the outer mitochondrial membrane including mitofuscin 2 (Mfn2), a protein responsible for mitochondrial fusion (Filadi, Pendin and Pizzo, 2018). Phosphorylation of Mfn2 signals Parkin translocation to the mitochondria which allows PINK1 to phosphorylate Parkin at serine65, thereby activating it. Parkin is an E3 ubiquitin ligase that is predominantly located in the cytosol, however once recruited to the mitochondria, Mfn2 serves as a receptor for Parkin bringing it in close proximity with the mitochondrial substrates, of which it then poly-ubiquitinates (Song, Mihara, Chen, Scorrano & Dorn, 2015). Poly-ubiquitination of the mitochondrial outer membrane proteins is recognized by sequestosom-1 (p62/SQSTM1), a protein that binds both LC3 of the autophagosome through its LC3-interacting region and ubiquitin residues via its ubiquitin associated domain. Recruitment of the autophagosome to the damaged mitochondria then initiates autophagic removal (Figure 1.5). Additionally, it was demonstrated that Parkin was not necessary for mitophagy induction, but rather enhanced the process.

This process of mitophagy is particularly imperative to neuronal health due to their post-mitotic nature. This in combination with their heavy dependence on oxidative phosphorylation for energy production, places a heightened susceptibility to mitochondrial dysfunction. Dysfunctional mitophagy is closely linked to autosomal-recessive forms of Parkinson's disease, forms of cancer and heart disease (Redmann, Dodson, Boyer-Guittaut, Darley-Usmar & Zhang, 2014).
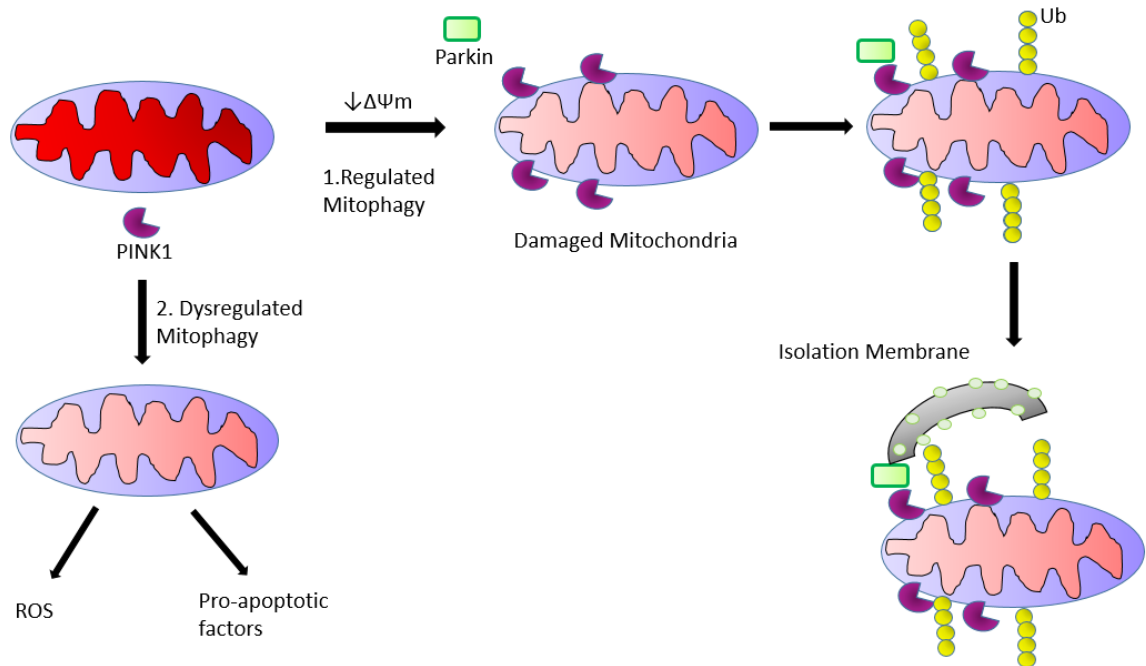
Figure 1.5 PINK1/Parkin Mitophagy Pathway: Under functional mitophagy program, PINK1 accumulates on the surface of depolarized mitochondria, as its import into the inner mitochondrial membrane is prevented. Upon accumulation, it recruits the E3 ubiquitin ligase Parkin, which acts to ubiquitinate various outer mitochondrial proteins. Polyubiquitination of the mitochondria targets the mitochondria for removal by the autophagosome, via interaction between autophagosomal-bound LC3 and ubiquitin-bound p62. Under dysregulated mitophagy, depolarized mitochondria are not targeted for removal and accumulate leading to the release of reactive oxygen species (ROS) and pro-apoptotic signals such as caspase 3.

1.6   Cerebral Ischemia

Defects in autophagy and mitophagy have been implicated in aging, diabetes and multiple NDs. Recently however evidence of autophagic induction during ischemic/hypoxic conditions has provoked the question of whether autophagy plays important roles during cerebral ischemia.

Cerebral ischemia is a form of stroke which is caused by insufficient blood flow to the brain resulting in reduced oxygen and glucose supply to neuronal tissue. There exist two main forms, global ischemia resulting from blocked blood flow to the entire brain and focal ischemia caused by occlusion of certain cerebral blood vessels (Tang, Tian , Yi , & Chen , 2016). Stroke is the third leading cause of death worldwide and the major cause of adult disability (Liu et al., 2014). When blood flow to the brain is blocked, cells undergo molecular changes including excitotoxicity, oxidative stress, mitochondrial dysfunction and inflammation all of which can lead to irreversible tissue damage and cell death. Researchers have identified three major pathways of ischemic cell death including necrotic, apoptotic and autophagocytotic cell death. Unlike necrosis and apoptosis which definitely lead to tissue injury, autophagy could potentially serve as a therapeutic target for ischemic brain injury. In 2017, Guo demonstrated that upregulation of hypoxia-inducible factor-1a (HIF-1a) a key transcription factor that regulates gene expression during hypoxic stress in a human cortical neuron cell line resulted in increased autophagy as well as reduced cell apoptosis (Guo, 2017). However, it is still controversial whether induction of autophagy/mitophagy during ischemia is neuroprotective or neurodegenerative. Additionally, the complexity of the autophagic pathway invites further investigation into the molecular players involved.

1.7   Tumour-protein-53-induced nuclear proteins 1 & 2

In recent years, two homologous proteins expressed only in higher eukaryotes have been described to play roles in mammalian autophagy and mitophagy. Tumour- protein 53-induced nuclear protein (Tp53INP1) also known as stress inducible protein (SIP) is a target gene of p53 that functions mainly to induce the expression of genes involved in cell cycle arrest and apoptosis and tumour-protein 53-induced nuclear protein 2 (Tp53INP2) also

known as diabetes and obesity regulated (DOR) gene, which has a bifunctional role as a modulator of autophagy and gene transcription. Both genes are highly conserved in mammals and are believed to have arisen through a gene duplication event from the ancestral TP53INP gene, found in Drosophila. Both proteins are ubiquitously expressed, with Tp53INP1 having greater expression in the lymphoid organs, and Tp53INP2 in highly metabolic tissue such as muscle and the CNS (Saadi, Seillier & Carrier, 2015). Key to their participation in autophagy are two highly conserved domains important nucleocytoplasmic shuttling (nuclear export signal (NES)) upon autophagy induction and permitting interaction with autophagy family proteins (LC3-interacting region (LIR)) (Sancho et al., 2012).

The Tp53INP1 gene encodes two different isoforms, Tp53INP1α and Tp53INP1β, which are identical except for an additional C-terminal region on Tp53INP1β. Regardless of the minor structural difference, there are no functional difference between the two isoforms to date. Tp53INP1α/β are both gene targets of p53, as well as transcriptional activators of p53. Their ability to influence p53 expression occurs through their interaction with kinases homeodomain-interaction protein kinase 2 (HIPK2) and protein kinase C delta (PKCδ), which in turn act to phosphorylate p53 creating a positive feedback loop (Seillier et al., 2012). Tp53INP1 is localized in sub-nuclear structures called promyelocytic leukaemia protein nuclear bodies (PML-NBs), of which is also believed to be the site that HIPK2 binds and phosphorylates p53. Through various gain of function and loss of function studies, Tp53INP1 was shown to be involved in cell cycle regulation, apoptosis, cell migration and adhesion and ROS regulation. Additionally, it plays a key role in cellular homeostasis by affecting autophagy by its binding to LC3. Studies have demonstrated that ectopic expression of Tp53INP1 promotes autophagy-dependent cell death. Interestingly, in 2015 a study demonstrated that immortalized mouse embryonic fibroblasts with knocked down Tp53INP1 expression had increased mitochondrial mass consistent with decreased levels of PINK1 and Parkin (Seillier et al., 2015). Additionally, because defective mitochondria produce increased ROS, this demonstrated that Tp53INP1 involvement in mitophagy is crucial to ROS regulation.

The paralog of Tp53INP1, Tp53INP2 has also been demonstrated to play an important role in autophagy through its interaction with autophagosomal proteins. In 2012, it was demonstrated that Tp53INP2 binds to LC3 and LC3-related proteins GABARAP and GABARAP-like2 in an autophagy-dependent manner, and that the absence of Tp53INP2 leads to less effective mTOR-dependent autophagy induction as indicated by a markedly reduced number of autophagosomes (Nowak et al., 2009). Ectopic expression of Tp53INP2 however does not significantly affect cell cycle arrest nor apoptosis, and therefore does not share the same functions as Tp53INP1. It does however share a functional role in transcription by serving as a coactivator of thyroid hormone receptor. Although Tp53INP1 does appear to affect autophagy similarly to Tp53INP2, the regulation of these proteins are different. For example, stressors will induce Tp53INP1 gene expression, however only cause Tp53INP2 translocation from the nucleus (Nowak, et al., 2012). Additionally, whether Tp53INP2 plays a role in mitophagy and ROS regulation is still not known. However there is evidence suggesting that both proteins may serves as dual regulators of autophagy, which could provide two potentially powerful gene targets (Sancho et al., 2012).

1.8   Objective of this Thesis

Neuronal autophagy plays a critical role in the homeostasis of neurons, and the maintenance of protein and organelle quality control. The post-mitotic nature of neurons necessitates an adequate balance between autophagosome formation and degradation. Any impairment in this balance or to the function of autophagy can be detrimental to neurons and contribute to neurodegeneration as seen in such disorders as Parkinson's disease and cerebral ischemia. Therefore, an understanding of the key regulators of neuronal autophagy, particularly during stress induction, is vital to understanding the mechanisms that underlie the of role autophagy in neurons, as well as shed light on what contributes to is dysregulation in the diseased neurodegenerative states. Tp53INP1 and Tp53INP2 are two homologous proteins of which have been demonstrated to play important roles in non-neuronal autophagy. There function in autophagy is mainly attributed to a highly conserved LIR domain which allows the proteins to bind directly to the autophagosomal membrane and the NES region which allows nucleocytoplasmic shuttling upon autophagy induction. Tp53INP1 has also been shown to participate in PINK1/Parkin mitophagy, however to date

there is no evidence of Tp53INP2's role during mitochondrial stress. The heavy reliance of neurons on autophagic and mitophagic processes, as well as evidence of the dysregulation of these processes in disease phenotypes, warrants the need to understand which molecular players regulate these processes. The objective of this thesis is to investigate whether Tp53INP1 and Tp53INP2 play roles in stress-induced neuronal autophagy, as well as determine if Tp53INP2, similarly to its homologue participates in mitophagy during mitochondrial stress or injury.

1.9　　Hypothesis

Tp53INP1 and Tp53INP2 are important regulator or neuronal autophagy, acting to promote autophagy in response to stress induction.

Chapter 2

2 Materials and Methods

2.1 Animals

All animal procedures were carried out according to the protocols approved by the Animal Care Committee at University of Western Ontario. Mice carrying targeted mutations for TP53INP1 were generated on a C57BL/6 background in the laboratory of Dr. Nelson Dusetti (Marseille, France) (Gommeaux et al., 2007). Transgenic mice were maintained on a C57BL/6 background and genotyped. Timed-pregnant CD1 mice were obtained from Charles River Laboratories (Sherbrooke, QC, CA).

2.2 Cell Culture

2.2.1 Primary Cortical Neurons

Primary cortical neurons were isolated from the cerebral cortices of embryonic day 14.5-15.5 (E14.5-15.5) fetuses that were dissected from timed pregnant TP53INP1 transgenic mice and C57BL/6 mice. Pregnant mice were euthanized via an intra-peritoneal injection of 700mg/kg sodium pentobarbital prior to cervical dislocation. Cerebral cortices were immediately dissected from individual embryos and following removal of the meninges were placed in individual tubes containing 1x Hanks' Balanced Salt Solution (HBSS) [Corning, lot #20-021-CV]. To dissociate the cortical neurons, the individual cortices were trypsinized with 1x HBSS solution supplemented with 1.2 mM $MgSO_4$ [Fisher, #M65-3] and 1x trypsin [Sigma, #T4549], and placed in a 37°C incubator on a rotor, for 25 minutes. Trypsinization was halted with 1x HBSS solution supplemented with 1.2 mM $MgSO_4$, 0.25 mg/ml DNase I, and 0.2 mg/mL trypsin inhibitor [Roche, #6365752001]. Next, the cell suspensions were centrifuged for 4 minutes at 400xg and the supernatant was carefully removed. The pellets were resuspended in 1x HBSS solution supplemented with 3 mM $MgSO_4$, 1.15 mg/mL trypsin inhibitor and 0.75 mg/mL DNase I. To ensure complete dissociation, the cells were triturated 10-14 times through a flame polished glass pipette and centrifuged at 400xg for 4 minutes. Following centrifugation, the supernatant was

aspirated and the cell pellets were resuspended in 2 mL complete neurobasal media (NBM) [Gibco, #21103-049] supplemented with 0.5x B27 [Life Technologies, #17504044], 1xN2 [Life Technologies, #17502048], 0.5x Glutamax [Life Technologie, #35050061] and 50 U/mL penicillin: 50μg/mL streptomycin [Life Tehcnologies, #15140-122]. Cell density was determined using 0.4% Trypan Blue [SigmaAldrich, #T8154] and a TC20^{TM} Automated Cell Counter [BioRad]. Cell suspensions were diluted with supplemented NBM to 6 x 10^5 cells/mL and plated in 35 mm (2mL; 1.2 x 10^6 cells/dish) Nunc dishes [Thermo Scientific] that were previously coated with poly-L-ornithine [Sigma, #P4957]. The cultures were maintained at 37°C with 5% CO_2.

2.2.2   Cerebellar Granule Neurons

Cerebellar granule neurons were isolated from the cerebellum of postnatal day 6 (P6) fetuses from timed pregnant TP53INP1 transgenic mice and C57BL/6 mice. Pups were euthanized by decapitation and the cerebellum was extracted immediately and dissected from individual pups and following the removal of the meninges were placed in individual tubes containing 1x Hanks' Balanced Salt Solution (HBSS) [Corning, lot #20-021-CV] . To dissociate the cerebellar neurons, the individual cortices were trypsinized with 1x HBSS solution supplemented with 1.2 mM $MgSO_4$ [Fisher, #M65-3] and 1x trypsin [Sigma, #T4549], and placed in a 37°C incubator on a rotor, for 25 minutes. Trypsinization was halted with 1x HBSS solution supplemented with 1.2 mM $MgSO_4$, 0.25 mg/ml DNase I, and 0.2 mg/mL trypsin inhibitor [Roche, #6365752001]. Next, the cell suspensions were centrifuged for 4 minutes at 400xg and the supernatant was carefully removed. The pellets were resuspended in 1x HBSS solution supplemented with 3 mM $MgSO_4$, 1.15 mg/mL trypsin inhibitor and 0.75 mg/mL DNase I. To ensure complete dissociation, the cells were triturated 10-14 times through a flame polished glass pipette and centrifuged at 400xg for 4 minutes. Following centrifugation, the supernatant was aspirated and the cell pellets were resuspended in 2 mL complete neurobasal media (NBM) [Gibco, #21103-049] supplemented with 0.5x B27 [Life Technologies, #17504044], 1xN2 [Life Technologies, #17502048], 0.5x Glutamax [Life Technologie, #35050061], 20 mM KCl and 50 U/mL penicillin: 50μg/mL streptomycin [Life Technologies, #15140-122]. Cell density was determined using 0.4% Trypan Blue [SigmaAldrich, #T8154] and a TC20^{TM} Automated Cell Counter [BioRad]. Cell suspensions were diluted with supplemented NBM to 6 x 10^5

cells/mL and plated in 35 mm (2mL; 1.2 x 10^6 cells/dish) Nunc dishes [Thermo Scientific] that were previously coated with poly-L-ornithine [Sigma, #P4957]. The cultures were maintained at 37°C with 5% CO_2.

2.2.3   Cell Lines

HeLa Cervical Cancer Cells. HeLa cells were generously provided by the Schild-Poulter Lab, and were maintained in Dulbecco's Modified Eagle Medium (DMEM) [Gibco, #11965118] supplemented with 10% Fetal bovine serum (FBS) [Gibco, #12483-020] and 0.1% penicillin-streptomycin (100 U/mL) [Sigma #P4333] in T-75 flasks and passaged every 2-4 days at a 1:10 dilution.

2.2.4   Cell Treatments

Cell transfection. For transient transfection experiments cells were plated in 12-well plates on coverslips that were coated with poly-D-lysine [Corning, #354210] (50ug/ml) at a density of 65,000 cells/well 24 h prior to transfection with Lipofectamine 2000 [Invitrogen, #11668-019] method (Invitrogen). Cells were transfected with 0.5-1.0ug/ml of plasmid DNA per well, using a 1:2.5 DNA: Lipofectamine 2000 ratio.

Tp53INP2 expression cell experiments were conducted in HeLa cells which were transfected with plasmids using Lipofectamine 2000. Cells were transfected with 0.5-1.0ug/ml of plasmid DNA per well, using a 1:2.5 DNA: Lipofectamine 2000 ratio. 24hrs after transfection cells were treated with carbonyl cyanide m-chlorophenyl hydrazone (CCCP) [Sigma, #C2759] for 6 hours and 24hours before being fixed with 4% paraformaldehyde for 30 mins and stained with Hoechst nuclear stain.

2.3   Genotyping

Genotyping was conducted by isolating genomic DNA from tail clips of each pup. Primers used to detect the TP53INP1 wild type and knockout alleles were 5'- AAT GTA TGC AAT CTT AGC TGA TGC-3' (forward) and 5'- CCA AAC ACT GTC ACT GTA TTG ATA-3' (forward) respectively, with a common reverse primer 5'- TCT TGA GGT AAC ATA GTG AAA TGC-3'. The list of PCR reagents can be found in Appendix B Table 3. The PCR cycling conditions includes cycling through the following steps for 32 cycles; 94°C

for 3 minutes, 94ºC for 45 seconds, 62ºC for 45 seconds, and 72ºC for 1 minute. Following this cycling the samples undergo a final step of 72ºC for 10 minutes.

2.4 Protein Extraction and Quantification

Whole cell extracts were isolated by removing culture media from adhered cells on 35mm dishes. Cells were washed twice with 1x PBS and 200uL Lysis buffer [200uL RIPA Lysis buffer [Sigma, #R0278], 2uL protease inhibitor cocktail [Sigma, #P8340-5mL], 2uL Phosphatase Inhibitor Cocktail 2 [Sigma, #P5726-1mL] were added to each culture dish. Cells were scraped into the lysis buffer and transferred to 1.5 mL microcentrifuge tubes and placed on ice for 30 minutes. Samples were centrifuged at 12,000xg for 15 minutes at 4ºC. The supernatant from each tube wasa transferred to a fresh 1.5 mL tubes were protein concentrations were determined by Pierce BCA Protein Assay Kit [Thermo Scientific, #23225].

2.4.1 Western Blot and Densitometry Analysis

The volume corresponding to 20 µg of protein was mixed with a volume of 5x Laemmli Buffer and β-mercaptoethanol (1:20 dilution) to obtain a 1:5 dilution of the buffer. The samples were boiled on a 100ºC heating block for 5 mins to reduce disulfide bonds and denature proteins. The samples were then cooled on ice for 2-3 minutes prior to being loaded onto 1.5mm 15% bis-acrylamide mini-gel (National Diagnostics, #EC-890] and run at 30-60 mA for 40-60 minutes. Proteins were then transferred to Immuno-Blot PVDF membrane [BioRad, #1620177], previously activated in 100% methanol through semi-dry electroblotting. The membrane was then incubated in blocking solution (5% milk (w/v) in 1x TBST) for 1 hour at room temperature. The blocking solution was the replaced with primary antibody diluted in blocking solution (5% milk (w/v) in 1x TBST) and incubated on an orbital shaker overnight at 4ºC. Primary antibodies used included rabbit polyclonal LC3B [1:500; Novus Biologicals #NB100-2220], monoclonal mouse anti-β-actin [1:10,000; SigmaAldrich #A5441], SQSTM1/p62 [1:1000, Cell Signaling #5114S], TP53INP2 [1:1000; Novus Biologicals #NBP2-13466], p53 DINP1 [1:1000; Novus Biologicals #NBP1-31694], Cyclophillin-b [1:1000; Abcam #ab16045]. Following overnight incubation, the membranes were incubated in secondary antibody diluted in blocking solution on an orbital shaker for 1 hr at room temperature. Secondary antibodies

used were horseradish peroxidase (HRP)-conjugated goat anti-rabbit IgG (H+L) [1:10,000; Biorad #1706515] and goat anti-mouse IgG (H+L)[1:10,000, Biorad #1706516]. The membrane was then washed with washing buffer [1xTBST; 100mL 10x Tris-buffered saline, 900mL ddH2O, 1 mL Tween20] 3 times for 15 mins to remove excess secondary antibody. The membrane was then coated with a 1:1 mixture of Clarity Peroxide Reagent and Luminol/Enhancer Reagent from Clarity Western ECL Substrate [BioRad, #1705060] for 5 mins, before being sandwiched between two transparent overhead projector sheets to image. Blots were developed with ChemiDoc™ MP Imaging System [BioRad] (Molecular Devices).

Chemiluminescent blots were imaged using Image Lab Software version 5.2 [BioRad]. The band analysis tool was used to select the bands of interest and quantify the representative protein band for each sample and protein of interest. Relative density was normalized to control β-actin or cyclophillin-β level in each lane, and percentage change from the control samples were calculated.

2.5   RNA Extraction and Quantitation

RNA was extracted from neuronal cultures using Trizol [Invitrogen, # 15596026] reagent, according to manufacturer's protocol. RNA concentration was quantified using NanoDrop 1000 Spectrophotometer [Thermo Fischer] (Molecular Devices).

2.5.1   Quantitative RT-PCR

RNA samples were diluted to 10 ng/µl in UltraPure™ DNAse/RNAse-free distilled H2O [Invitrogen, # 10977023]. Primer probes were designed for ribosomal S12 which served as a reference gene, and for TP53INP1. Primer sequences used for probing TP53INP1 were 5'-   TGACTTCATAGATACCTGCCC-3'   (forward)   and   5'-TCACTGGTGTCAGTCAAGCA-3' (reverse) [SigmaAldrich], and for S12   5'-GGAAGGCATAGCTGCTGG-3'   (forward)   and   5'-CCTCGATGACATCCGACATCCTTGG-3' [SigmaAldrich]. QuantiFast SYBER Green PCR kit [Qiagen, #204154] was used, in which 40ng of RNA was mixed with 21 µL of MasterMix. Reagents and cycling conditions can be found on Appendix B. Samples were run in CFX Connect™ Real-Time PCR Detection System [BioRad] (Molecular Devices). Cycle threshold (Ct) and melt curves were analyzed using CFX Manager™ Software

[Biorad]. The change in mRNA transcript level was measured by comparing the fold change in treated samples relative to untreated controls. Fold change was measured by calculating ΔCt (treated sample- untreated control) and ΔΔCt (ΔCt Target Gene - ΔCt Housekeeping Gene), and finally $2^{-(\Delta\Delta Ct)}$.

2.6 Hypoxia Conditions

Primary cortical neurons extracted from embryonic day 14.5-15.5 mice, were subjected to hypoxic conditions after five days *in vitro*. These neurons were treated with 25 µM chloroquine, and then transferred to a humidified hypoxia glove box chamber that continuously exposed them to 0.5% O_2 and 5% CO_2 and maintained a 37°C environment for respective periods of time. Control cultures were kept at normoxic conditions of 20% O_2 and 5% CO_2 at 37°C.

2.7 Oxygen-glucose Deprivation Conditions

Primary cortical neurons extracted from embryonic day 14.5-15.5 mice, were subjected to hypoxic conditions after five days *in vitro*. Primary neurons were stripped of their conditioned media (which was collected and maintained for later) and incubated in oxygen-glucose deprived (OGD) media (in mmol/L: 116 NaCl, 5.3 KCl, 0.8 $MgSO_4$, 1.0 Na•H_2PO_4, 1.8 CaCl•$2H_2O$, 20 $NaHCO_3$, 0.02 Phenol Red) containing 25 µM chloroquine, and then transferred to a humidified hypoxia glove box chamber that with 0.5% O_2 and 5% CO_2 and maintained a 37°C environment for 2 hours. After the 2 hours incubation, primary neurons underwent reperfusion when the OGD media was removed and replaced with the conditioned media that was collected prior to OGD, which contained 25 µM chloroquine. The neurons were then incubated at normoxic conditions (20% O_2 and 5% CO_2) for the respective time periods.

2.8 Immunofluorescence Staining

Neurons were fixed in 4% PFA (containing 0.2% picric acid in 0.1M phosphate buffer, pH 7.1) for 30 mins before being washed with 1x phosphate buffered saline (PBS) and stained with Hoechst 33342 (0.25 µg/ml) dye. Neurons were then washed 3 times with ice-cold 1x PBS while gently rotating on an orbital rotator for 5 mins per wash. Neurons were then

incubated in 100% ice-cold methanol (-20°C) for 5 mins at RT in order to permeabilize the cells. They were then washed 3x with ice-cold 1xPBS for 5 minutes per wash while gently rotating. They were then incubated in blocking solution (2% BSA in 1xTBST) for 1 hour at RT. LC3 antibody (Cell Signalling; #2775S) was diluted in 2% BSA (1:100) that also contained MAP2 (Abcam, #11267) placed on coverslips. Dishes were incubated overnight at 4°C. The following day, neurons were washed 3x with RT 1x PBS for 5 minutes per wash with gentle rotation. They were then incubated in secondary antibody Goat-anti-rabbit Alexa 488 [at a 1:200, Invitrogen #A-11034] and Goat-anti-mouse 568 Phalloidin [a 1:200, Invitrogen #A12380] in 2% BSA in the dark at RT for 2 hrs. After incubation cells were washed 2 times in RT 1x PBS and once in UltraPure™ DNAse/RNAse-free distilled H2O for 5 minutes while gently rotating. They were then air dried before mounting on a slide using 10 μl Shandon™ Immu-Mount™. [ThermoScientific, #9990412].

2.8.1 Imaging and Analysis

Slides were imaged using the Leica SP8 confocal microscope. Slides were imaged at 40x objective and 1x zoom. All slides were imaged on the same day, a few hours after the coverslips were mounted. Laser power and percentage gain were kept consistent between all of the slides, regardless of any variations in staining. Processing involved adjusting the exposure of each RGB setting to eliminate background staining, and these optimal values were applied to every image to maintain consistency and remove any bias. Image were then quantified using ImageJ's RGB measure, in which the mean RGB of the entire field was measured. Because no dead cells contained LC3 punctae, the value for the green measure was divided by the total number of live cells to obtain the mean fluorescence per cell. A minimum of ten fields per slide were quantified per sample.

2.9 Statistical Analysis

All statistical analyses were computed using GraphPad Prism5 (GraphPad Software). Data was reported as the mean and standard error of the mean (SEM). Differences between groups were demonstrated using ANOVA with *post-hoc* Tukey's test and t-test. Statistical significance was quantified as *p*-value <0.05

Chapter 3

3   Results

3.1   Trophic deprivation of cerebellar granule neurons results in autophagy induction

Tp53INP1 has been implicated in playing a role in the regulation of nutrient deprivation-induced autophagy in non-neuronal cells, however its role in neuronal autophagy has yet to be investigated. The importance of adequately functioning autophagy in neuronal homeostasis has been effectively demonstrated, therefore in order to understand if Tp53INP1 plays a role in regulating this process, we elicited the use of two potent autophagy inducing paradigms; trophic factor deprivation and hypoxia.

Previous studies have demonstrated that the survival of cerebellar granule neurons (CGNs) in vitro is dependent on chronic depolarization. For this reason, CGNs are routinely cultured in depolarizing K^+ concentrations of 25 mM (K25). These high K^+ concentrations results in chronic depolarization that causes the release of glutamate, an excitatory neurotransmitter. This glutamatergic stimulation is said to mimic *in vivo* interactions with the cerebellar mossy fibers, particularly during development. Additionally, it was demonstrated that elevated K^+ in the culture medium promoted the maturation and survival of CGNs in culture (Balázs, Gallo and Kingsbury, 1988). Therefore when CGNs are switched to low potassium medium, (5 mM (K5)), they undergo potassium deprivation, which results in autophagy induction and cell death (Maycotte, Guemez-gamboa, & Moran, 2010). This model of trophic factor deprivation-induced neuronal apoptosis is believed to mimic aspects of de-innervation common in neuronal injury and neurodegeneration (Ambacher et al., 2012). Additionally, it was demonstrated that CGNs undergoing apoptosis showed increased levels of cathepsin L, a lysosomal endopeptidase as well as an increase in autophagosome structures (Kaasik, Rikk, Piirsoo, Zharkovsky, & Zharkovsky, 2005). Inhibition of autophagy with 3-methyladenine (3-MA) resulted in partial protection from potassium deprivation-induced apoptosis. Therefore, we used

trophic factor deprivation in CGNs to determine if Tp53INP1 plays a role in neuronal autophagy.

3.1.1 Assessing the effect of trophic deprivation on CGNs using varying lysosomal inhibitor concentrations

Since autophagy is a dynamic process, many autophagic studies elicit the use of lysosomal inhibitors to inhibit autophagosome turnover and capture autophagic flux, from cargo sequestration to lysosomal delivery. Unlike Bafilomycin A1 (Baf A1) which serves to inhibit the vacuolar H^+ ATPase of the lysosome to prevent its acidification, chloroquine (CQ) is a lysomotrophic weak base that enters the lysosome and becomes protonated, therefore changing the lysosomal pH (Redmann et al., 2017). We began by determining the kinetics of K5 induced autophagy in the presence of the lysosomal inhibitors Baf A1 or CQ on CGNs extractes from CD1 mice. We carried out trophic factor deprivation by replacing the conditioned media that the cells were cultured in (25 mM KCl) for 7 days with K5 media (5 mM) containing lysosomal inhibitors. In using these inhibitors, we expected that increased levels of autophagy over time would result in increased accumulation of LC3-II. As shown in Figure 3.1A, we found that lower concentrations of Baf A1 (25 nM) did not result in increases in LC3-II levels as expected, and that higher concentrations (50 nM) were toxic to the cells resulting in cell death, particularly at longer duration. However, exposure to K5 media in the presence of CQ at both 5uM and 8uM resulted in an increase in LC3-II with increased duration in K5 media. Therefore, in proceeding with our paradigm, we used 5 μM CQ. In addition to this, we did not see marked increases in basal levels of autophagy when cells were incubated at K25 conditions with CQ. This ensured that any increases that were observed during K5 conditions, were not solely due to the application of a lysosomal inhibitor but moreover a result of trophic deprivation. Furthermore, by evaluating nuclear morphology using Hoechst staining, we observed over 50% of a decrease in percentage survival in cells that had undergone 12 hours of K5 treatment (Figure 3.2B). Therefore, in further studies we restricted our analysis of autophagic flux to 6 hours which preceded the onset of apoptotic cell death (Figure 3.3).
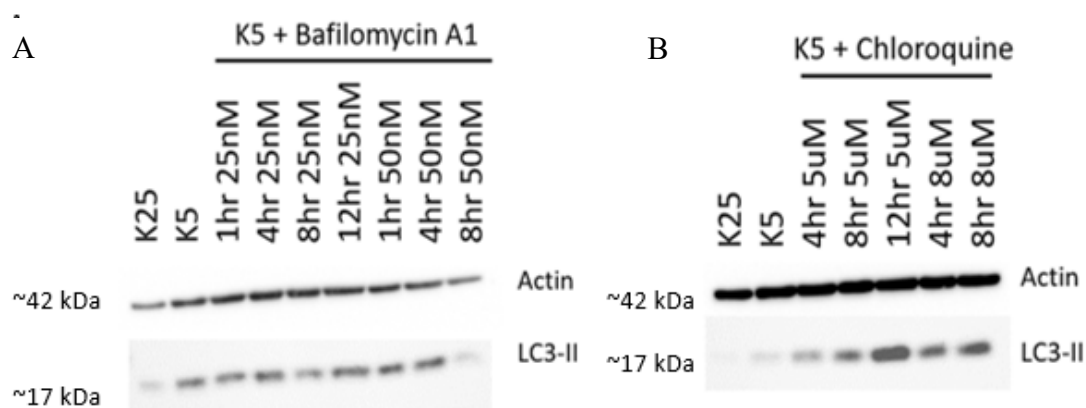
Figure 3.1. The effect of lysosomal inhibitors bafilomycin A1 and chloroquine on LC3-II levels in cerebellar granule neurons subjected to K5 treatment. To determine the kinetics of the effect of K5 treatment on autophagy, cerebellar granule neurons were treated with high and low doses of bafilomycin A1 (*A*) and chloroquine (*B*) for up to 12 hours. Western blot analysis was used to determine the effect of both lysosomal inhibitors on blocking autophagic flux, by blotting for LC3-II.

A

K25　　　　　　　　　　　　　　K5 12h
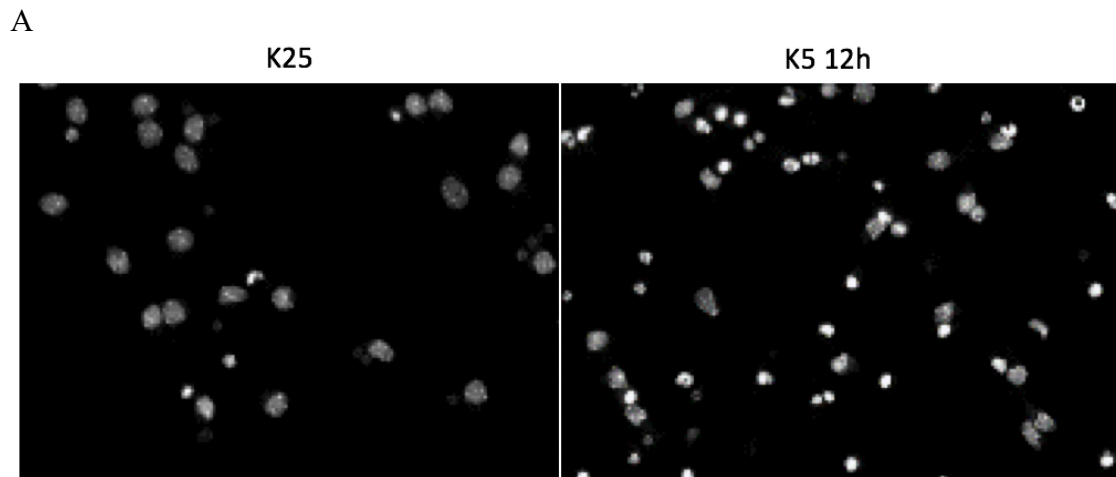
B
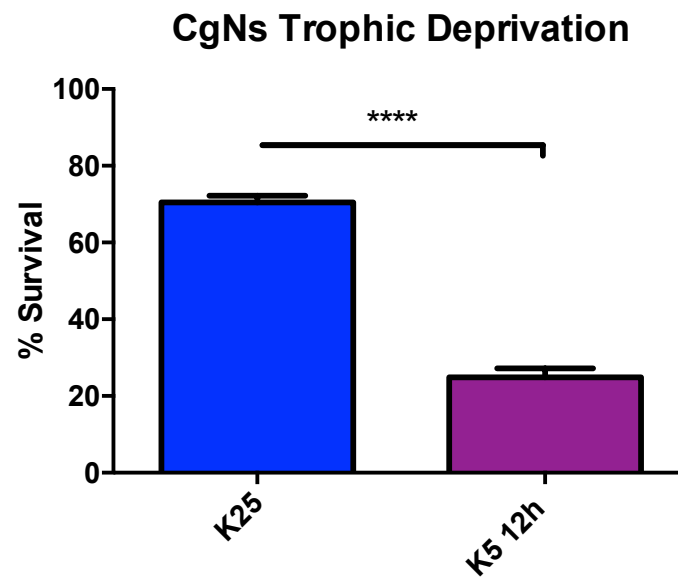
Figure 3.2. Percent survival of cerebellar granule neurons undergoing 12 hours of trophic deprivation. CGNs were subjected to 12 hours of K5 treatment. *A.* Cells were stained with Hoechst nuclear stain and examined for apoptotic morphology. *B.* Quantitation of percent survival was measured by dividing the number of live cells in each field by the total number of live and dead cells. Data is shown as mean ± SEM of 3 independent experiments.
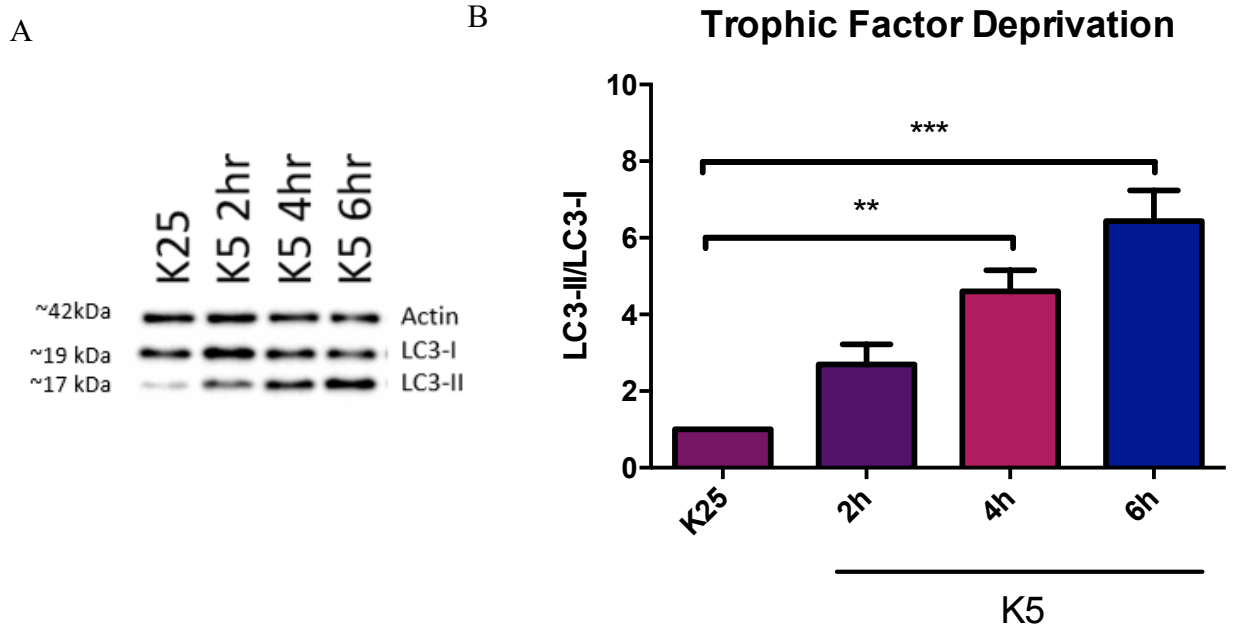
Figure 3.3. Cerebellar granule neurons subjected to trophic deprivation (K5) display increased levels of autophagy as measured by LC3-II/LC3-I ratio. Cerebellar granular neurons (CGNs) extracted from P7 mice were cultured for 5 days and either maintained in cultured media containing 25 mM potassium (K25) or switched to media containing 5 mM potassium (K5) and 5 µM CQ. *A.* Representative western blot depicting changes in LC3 levels in CGNs incubated in K5 media for up to 6 hours. *B.* Graphical representation demonstrating increased conversion of LC3-I to LC3-II with greater time in K5 media as well as increased LC3-II levels. Data is shown as mean ± SEM of 4 independent experiments. **$p<0.01$ and ***$p<0.001$ in one-way ANOVA.

3.2 Tp53INP1-deficient cerebellar granule neurons experience significantly attenuated autophagy induction in response to trophic deprivation

Since we saw robust increases in autophagy during trophic deprivation of cerebellar granule neurons from CD1 mice, we used trophic deprivation to determine if Tp53INP1 plays a role in neuronal autophagy. When we subjected wild-type and Tp53INP1-defiicent CGNs to potassium deprivation, we observed the level of autophagy increase with increased duration of the trophic deprivation, from 2 to 6 hours, showing significant increases from control at 4 and 6 hours (**p<0.01 and ****p<0.0001, respectively). This was measured by western blot analysis of changes in the conversion of cytosolic LC3 (LC3-I) to autophagosome membrane-bound LC3 (LC3-II). However, Tp53INP1-deficient neurons demonstrated significantly reduced autophagy at 6 hours compared to that of the wild type controls (Figure 3.4).

In its inactivated form LC3-I appears diffusely dispersed throughout the cytosol. However, upon autophagic induction LC3 becomes conjugated with the autophagosomal membrane, and therefore accumulates in regions called puncta when visualized using immunofluorescence. The formation of punctae structures are indicative of autophagosome formation and therefore autophagy induction. It is therefore used as a reliable tool to visualize autophagy. We used immunofluorescence to measure LC3-II protein content and distribution in the cells, in order to determine whether differences in LC3 puncta exist between CGNs extracted from Tp53INP1$^{+/+}$ and Tp53INP1$^{-/-}$ mice. After K5 treatment, CGNs were fixed and probed for LC3. Images were taken using the Leica SP8, using identical % Gains and laser power, and analyzed using ImageJ. As depicted in Figure 3.5, Tp53INP1$^{-/-}$ neurons display fewer, less pronounced LC3 puncta (green) per cell than Tp53INP1$^{+/+}$ following exposure to K5 media in comparison to CGNs from Tp53INP1$^{+/+}$ mice.

A
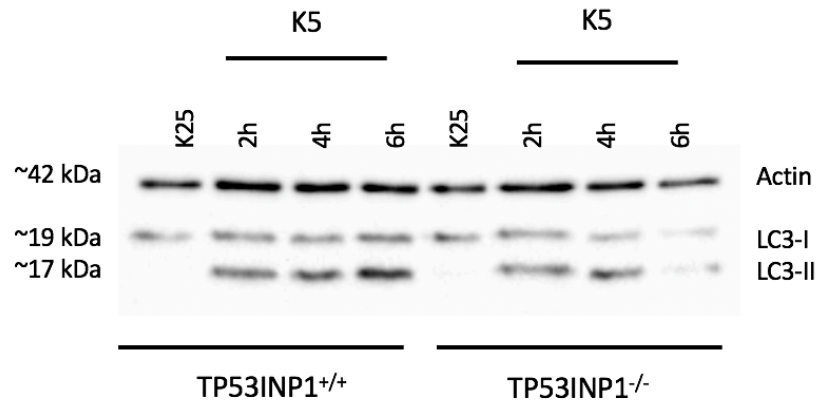
B

Figure 3.4. Tp53INP1-deficient cerebellar granule neurons show reduced induction in trophic deprivation induced autophagy. Cerebellar granule neurons extracted from (P7) Tp53INP1$^{+/+}$ and Tp53INP1$^{-/-}$ mouse pups underwent a media switch from media containing 25 mM potassium (K25) to media containing 5 mM potassium (K5) with 5 µM CQ for up to 6 hours. *A.* Representative western blot of LC3-I and LC3-II protein extracted from Tp53INP1$^{+/+}$ and Tp53INP1$^{-/-}$ CGNs. *B.* Graphical representation of the western blot depicting LC3-I and LC3-II protein ratios normalized to actin . The graph depicts increasing levels of autophagy induction in the wildtype CGNs with increasing time of K5 exposure, . Additionally, at 6 hours K5 there is a significant reduction in the level of autophagy in the Tp53INP1 deficient neurons in comparison to the wildtypes. Data is shown as mean ± SEM of 3 independent experiments. **p<0.01in two-way ANOVA.
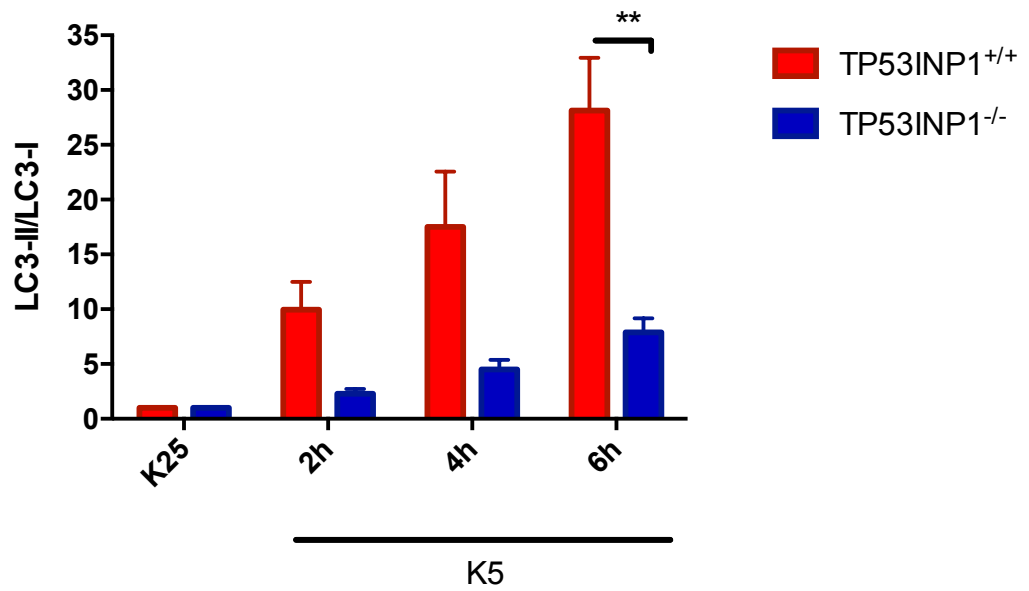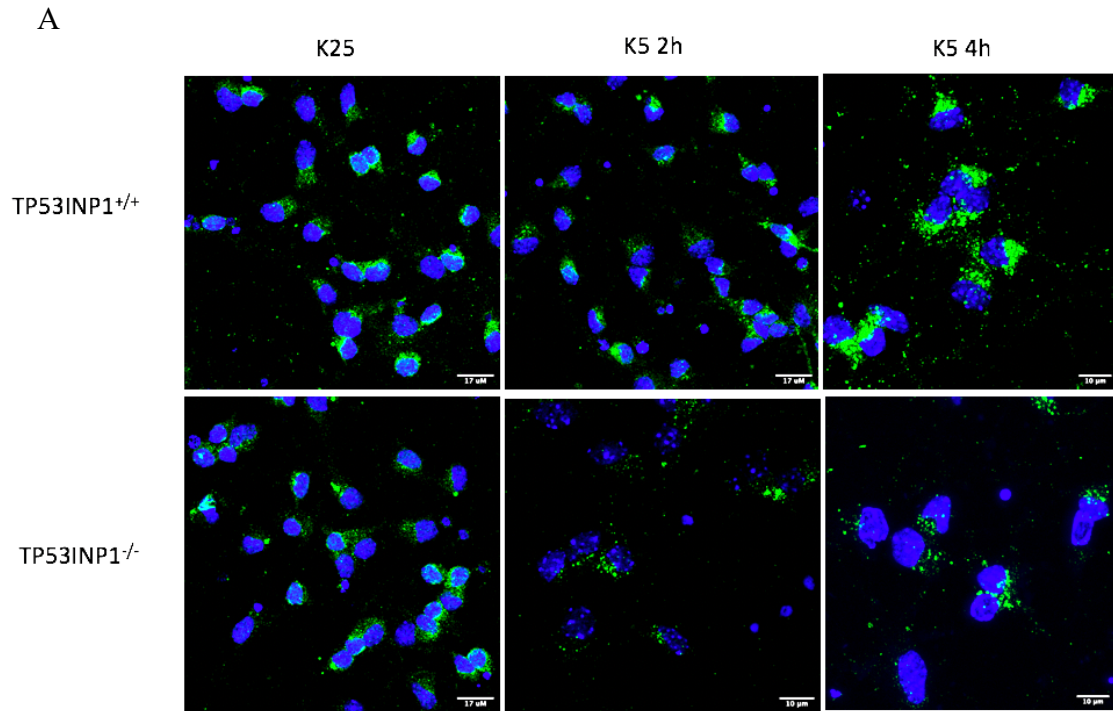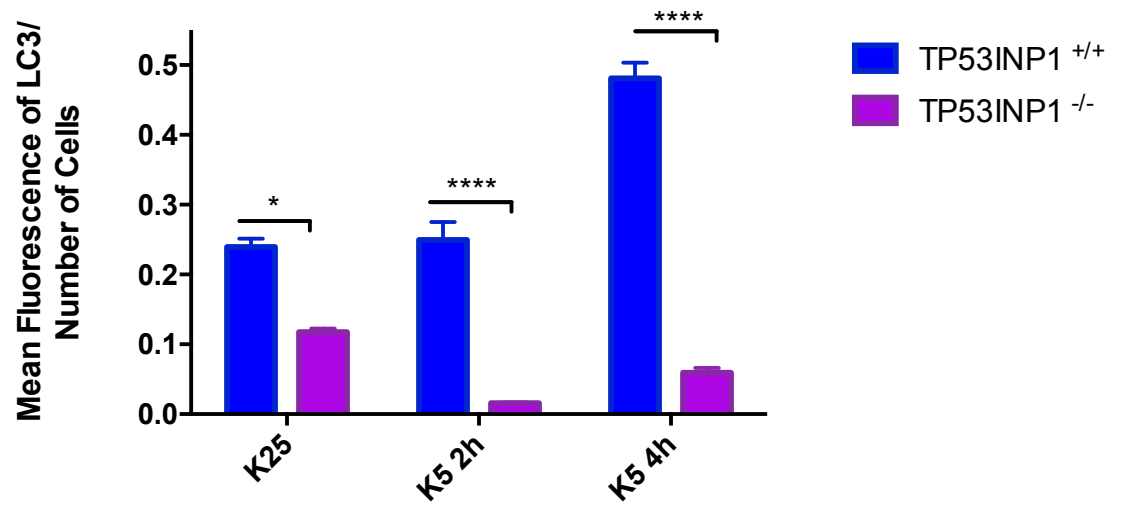
A

B

Figure 3.5. Tp53INP1-deficient cerebellar granule neurons display reduced trophic deprivation-induced autophagy. Cerebellar granule neurons extracted from P7 Tp53INP1$^{+/+}$ and Tp53INP1$^{-/-}$ mice were cultured for 5 days and then maintained in media containing 25 mM potassium (K25) or switched to media containing 5 mM potassium (K5) for 4 hours. CGNs were fixed and probed for LC3 by immunofluorescence . *A.* CGNs immunostained for LC3 (green) and counterstained with Hoechst dye (blue). Tp53INP1$^{+/+}$ neurons (top row) demonstrate more pronounced puncta formation and less diffuse cytosolic expression with increased incubation in K5 media. Tp53INP1$^{-/-}$ neurons demonstrate dramatically less puncta formation compared to the wild-types. *B.* Graphical representation of mean fluorescence of LC3 expression per cell, demonstrating significant decreases in autophagy induction in basal and stressed conditions in Tp53INP1$^{-/-}$ compared to wildtypes. Fluorescence was measured using ImageJ RGB Measure by determining the average fluorescence for each wavelength per field and normalized for the total number of cells in each field. Data is shown as the mean ± SEM from 3 different pups. *p<0.05 and ****p<0.0001 in two-way ANOVA. Scale is equal to 17 um and 10 um.

3.3 Hypoxic stress activates autophagy induction in primary cortical neurons

In order to investigate the role of Tp53INP1 in a second model of neuronal autophagy we used a hypoxia paradigm in primary cortical neurons (PCNs), as oxygen-deprivation is one of the most established inducers of autophagy (Fang, Tan, & Zhang, 2015). Previous studies have demonstrated that hypoxia-induced autophagy in early stages can be neuroprotective, however when prolonged can promote cell death. Therefore, in order to observe the effect of hypoxic injury on neuronal cells, we began by subjecting PCNs extracted from CD1 embryonic day 14 mice to hypoxic conditions for up to 8 hours. These non-transgenic CD1 mice were initially used to determine the period of hypoxic exposure necessary for neurons to display an autophagic response. Autophagy was analyzed by measuring the conversion of LC3-I to LC3-II through western blot analysis. As shown in

Figure 3.6, we observed significant increases in autophagy induction as hypoxic exposure was increased from 2 to 8 hours.
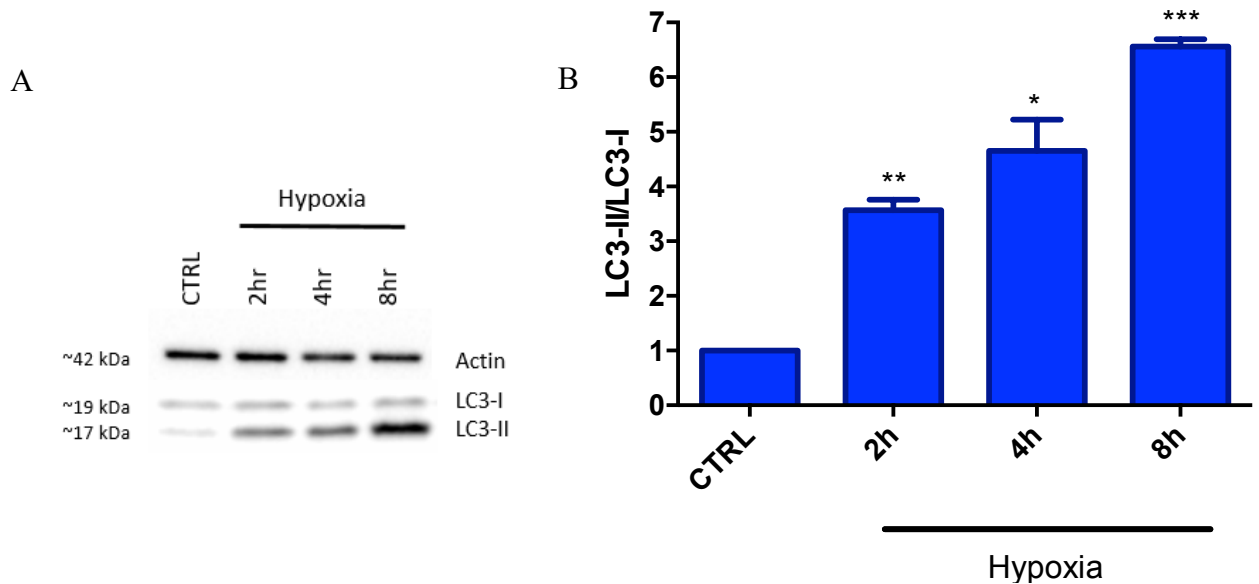
Figure 3.6. Hypoxic stress induces significant autophagy induction. Primary cortical neurons were subjected to hypoxic conditions of 0.5% O2 for up to 8 hours to determine the kinetics of autophagy induction. *A.* Western blot analysis was used to measure the change in cytosolic LC3 (LC3-I) to autophagosomal membrane LC3 (LC3-II) to determine the level of autophagy. *B.* Assessment of the LC3-II/LC3-i ratio, demonstrating the level of autophagy taking place. Autophagy induction begins as early as 2 hours of oxygen deprivation, and increases steadily for up to 8 hours Data is shown as mean ± SEM of 4 independent experiments. *p<0.05. **p<0.01 and ***p<0.001 in one-way ANOVA.

3.4 Hypoxia induced autophagy is attenuated in Tp53INP1-deficient cortical neurons

To investigate further into determining whether Tp53INP1 plays a role in neuronal autophagy we subjected PCNs extracted from Tp53INP1$^{+/+}$ and Tp53INP1$^{-/-}$ embryonic day 14 mice and cultured for 7 days to hypoxic conditions for up to 8 hours. As shown in Figure 3.7, PCNs from Tp53INP1$^{+/+}$ pups show significant increases in LC3-I to LC3-II conversion at 2, 4 and 8 hours of hypoxic exposure (*$p<0.05$, ***$p<0.001$, ****$p<0.0001$ respectively), similar to what was observed in non-transgenic CD1 mice. However, in the PCNs from Tp53INP1$^{-/-}$ pups, the increase in LC3-II is significantly less compared to wildtype littermates at 4 and 8 hours of hypoxia, suggesting that the loss of Tp53INP1 is attenuating the cells autophagic response to hypoxic stress.

In addition to western blotting we used immunofluorescence to examine the protein content and distribution of LC3-II within PCNs from Tp53INP1$^{+/+}$ and Tp53INP1$^{-/-}$ pups. Due to limitations involving the availability of PCNs, we were only able to compare PCNs from Tp53INP1 present and deficient pups for 8 hours of hypoxic conditions. For this assay we opted for 8 hours of hypoxia, as based on our findings LC3-II protein levels increase during increased hypoxic exposure, therefore we expected to see the evident changes in LC3 staining as well at this time point. Cells were fixed and probed for LC3. Images were taken using the Leica SP8, using identical % Gains and laser power, and analyzed using ImageJ. As depicted in Figure 3.8, PCNs from Tp53INP1 deficient mice reduced LC3 expression in comparison to Tp53INP1 present PCNs, further suggesting that the absence of Tp53INP1 attenuates stress-induced autophagy.

A

TP53INP1 +/+   TP53INP1 -/-

Control 2hr 4hr 8hr Control 2hr 4hr 8hr

~42 kDa   Actin
~19 kDa   LC3-I
~17 kDa   LC3-II

B

LC3-II/LC3-I

TP53INP1 +/+
TP53INP1 -/-

Duration of Hypoxia
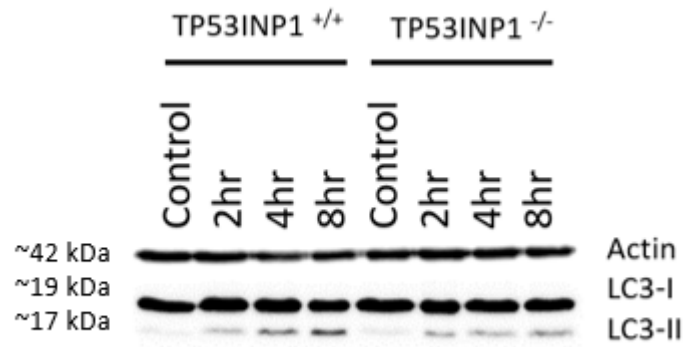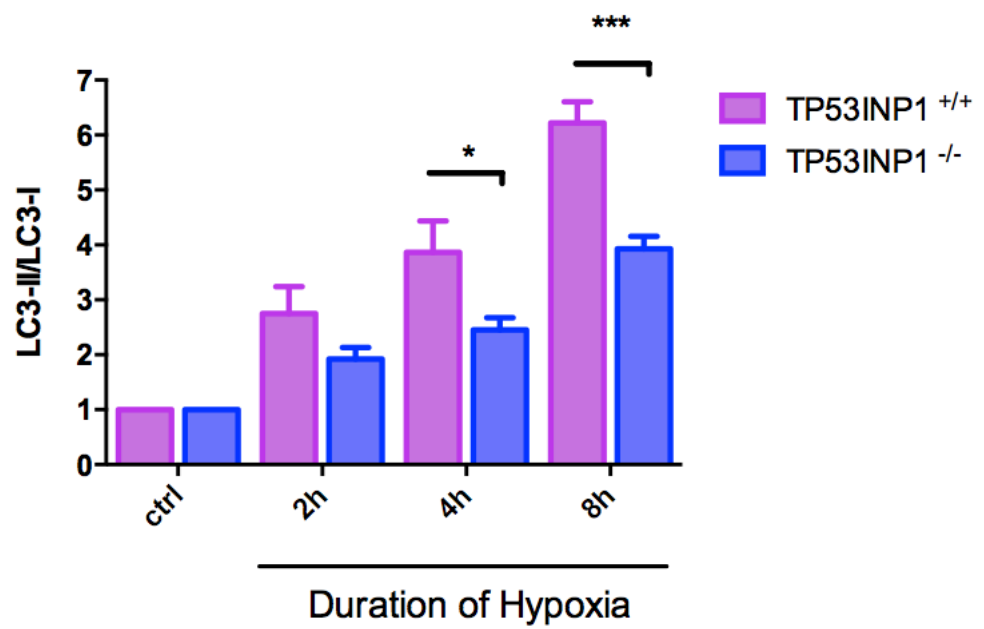
Figure 3.7. Autophagy induction in response to hypoxic stress is attenuated in Tp53INP1$^{-/-}$ PCNs. PCNs from Tp53INP1$^{+/+}$ and Tp53INP1$^{-/-}$ embryonic day 14 pups were subjected to hypoxic conditions of 0.5% O2 and 5% CO2 for either 2, 4 or 8 hours and protein levels of LC3-II/I were determined by western blot analysis. *A.* Representative western blot demonstrating changes in autophagy as measured by the conversion of cytosolic LC3-I to autophagosomal LC3-II that occurs from 2 hour to 8 hours in the wildtype PCNs is not observed in the Tp53INP1- deficient PCNs, thereby suggesting a reduction in autophagy in the absence of Tp53INP1. *B.* Graphical representation of LC3-I/LC3-II ratio was quantified using ImageLab. Data is shown as mean ± SEM of 3 independent experiments. *p<0.05 and ***p<0.001 in two-way ANOVA.

A

TP53INP1$^{+/+}$ TP53INP1$^{-/-}$
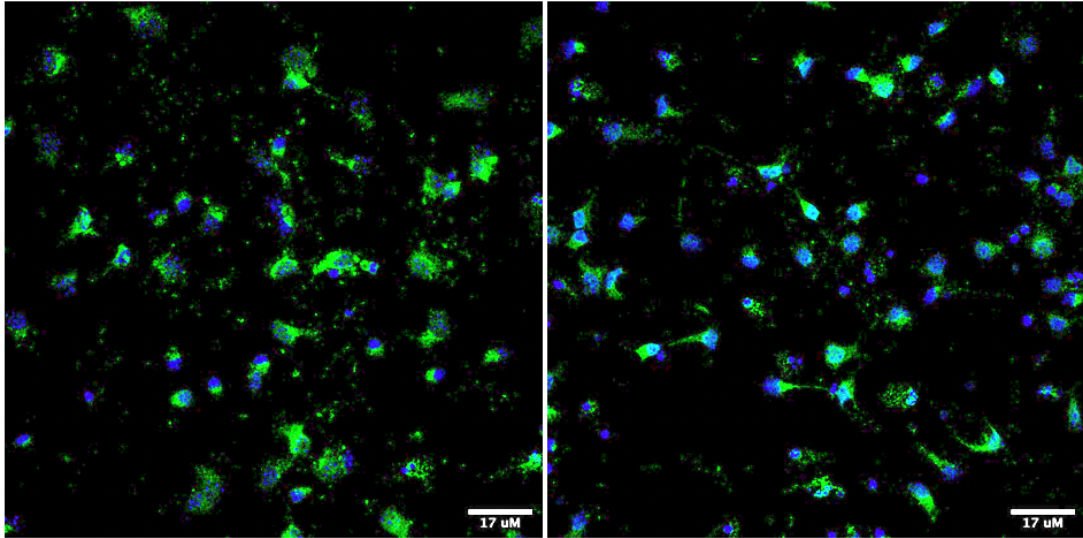
B
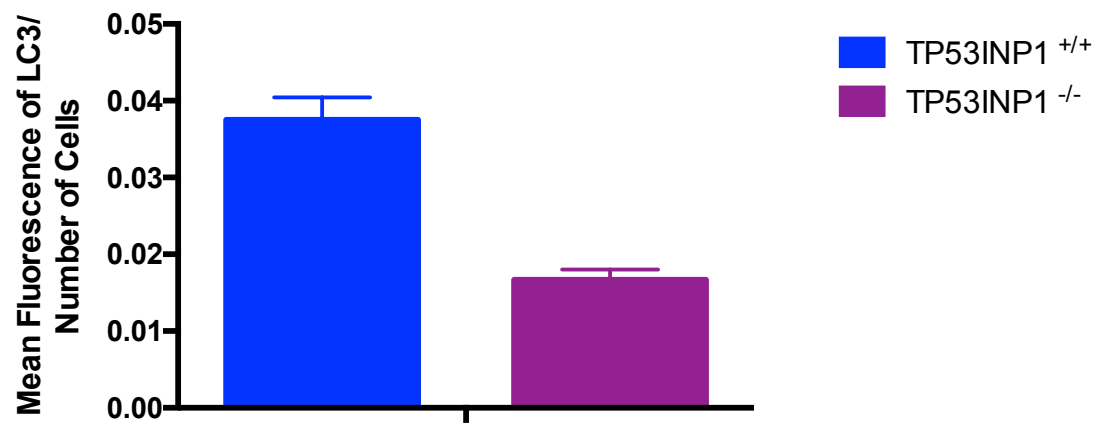
Figure 3.8. Immunofluorescence staining of LC3 in Tp53INP1 deficient PCNs demonstrate reduced hypoxia-induced LC3 expression. PCNs extracted from Tp53INP1$^{+/+}$ and Tp53INP1$^{-/-}$ mice were subjected to hypoxic conditions of 0.5% O2 and 5% CO2, then fixed and probed for LC3 (green) and stained with Hoechst nuclear stain (blue). Tp53INP1$^{+/+}$ neurons demonstrate more pronounced LC3 punctae after 8 hours hypoxic exposure compared to Tp53INP1$^{-/-}$ *B.* Graphical representation of mean fluorescence of LC3 expression per cell, demonstrating significant decreases in autophagy induction in basal and stressed conditions in Tp53INP1$^{-/-}$ compared to wildtypes. Fluorescence was measured using ImageJ RGB Measure by determining the average fluorescence for each wavelength per field and normalized for the total number of cells in each field. Data is shown as the mean ± SEM from 2 different pups. Scale is 17um.

3.5 Oxygen-glucose deprivation and reperfusion results in increased autophagy induction

Recently evidence of autophagic induction during ischemic/hypoxic conditions has provoked the question of whether autophagy plays important roles during cerebral ischemia. Hypoxia appears to regulate autophagy pathways differently depending on the severity and duration of the insult. Regardless of this, oxygen deprivation is one of the most established stimuli for autophagy induction and serves as a physiologically relevant model in both laboratory and clinical settings. We modelled ischemic injury and reperfusion by incubating PCNs from CD1 E14 mice in oxygen-glucose deprived (OGD) media and hypoxic conditions for 2 hours, prior to replacing the media with the previously conditioned media and placing the cells in normoxic conditions, respectively. We monitored the level of autophagy for up to 24 hours reperfusion (RP) and found that autophagy was stimulated immediately following OGD at 0 hours and increased significantly at 4 and 8 hours as measured by both the conversion of LC3-I to LC3-II (Figure 3.9). Therefore, OGD for up to 8 hours results in increases in autophagic induction.

A
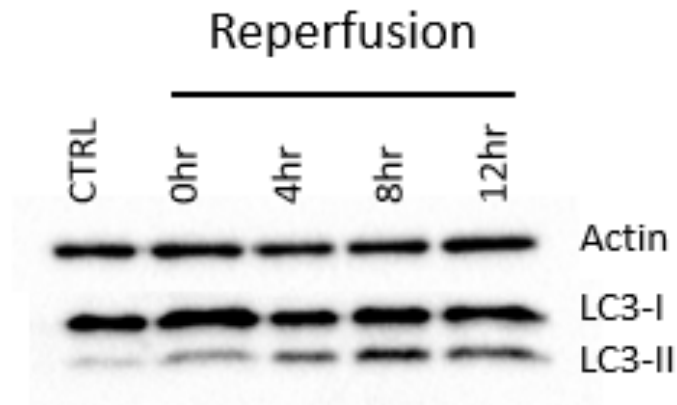
B
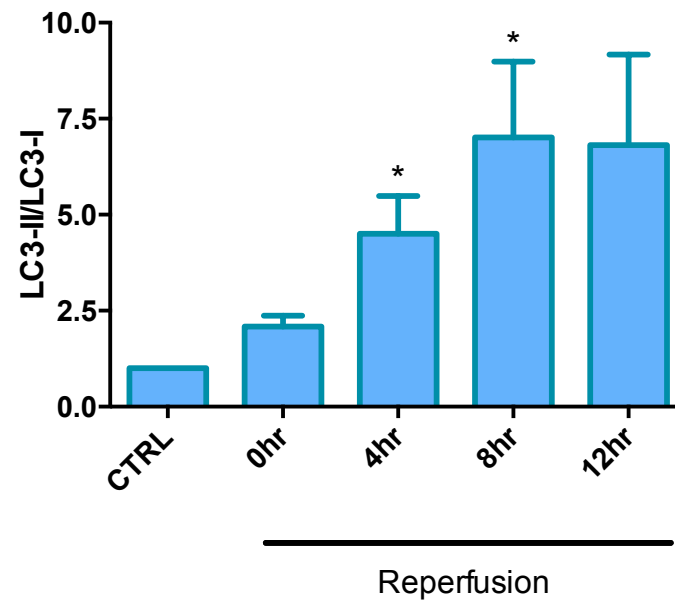
Figure 3.9. Primary cortical neurons subjected to oxygen-glucose deprivation conditions show autophagy induction up to 8 hours. Primary cortical neurons extracted from embryonic day 14 mice underwent oxygen-glucose deprivation (OGD) by replacing media with glucose-free buffer while being subjected to 2 hours in hypoxic conditions of 0.5% O2 and 5% CO2. After the 2 hours, the cell underwent reperfusion by replacing buffer with previously conditioned media, and incubating in normoxic conditions (20% O2 and 5% CO2) for various periods of time. *A.* We used western blot analysis to observe changes in LC3-I and LC3-II levels. *B.* Graphical representation of western blots. quantitation for three different western blots. Data is shown as the mean ± SEM from 3 different experiments. *p<0.05 in student's t-test.

In summary, we demonstrate that neurons deficient in Tp53INP1, experience attenuated stress-induced autophagy in response to such physiological stressors such as trophic deprivation during neuronal injury, and hypoxic conditions that arise during cerebral ischemia. These findings suggest that Tp53INP1 plays an important role in stress-induced neuronal autophagy.

3.6 Tp53INP2 responds to mitophagy induction via nucleocytoplasmic shuttling to co-localize with the autophagosome

Previous work has demonstrated that Tp53INP2 participates in mTOR-dependent autophagy (Mauvezin, Sancho, Ivanova, Palacin, & Zorzano, 2012; Nowak, et al., 2012). This was attributed to its ability to shuttle out of the nucleus and interact with autophagy related proteins in response to mTOR inhibition. In addition to this it has been observed that mouse embryonic fibroblasts (MEFs) deficient in Tp53INP1, the homolog of Tp53INP2, display less effective mitophagy leading to the accumulation of damaged mitochondria and increased ROS production (Seillier, et al., 2015). However, it had yet to be determined whether Tp53INP2 also participates in mitophagy. Therefore, before investigating the role of Tp53INP2 in neuronal autophagy, we began by determining whether it plays a role in mitophagy in non-neuronal cells.

Since previous studies were conducted primarily in HeLa cells, we too utilized these cells to investigate whether Tp53INP2 responds to mitochondrial stress induction. We began by treating HeLa cells with carbonyl cyanide m-chlorophenyl hydrazine (CCCP), an established mitophagy inducer. CCCP is an ionophore that functions by uncoupling the mitochondrial proton gradient and depolarizing the inner mitochondrial membrane. It was previously demonstrated that 6 hours of CCCP treatment resulted in mitochondrial network fragmentation, and when prolonged to 24 hours resulted in complete loss of mitochondrial marker TOM 20 (Villa, et al., 2017).

Often times, the translocation of Parkin to depolarized mitochondria is used as a reliable indicator or mitophagy induction (Wang, Nartiss, Stiepe, McQuibban, & Kim, 2012). This is due to Parkin's role in mitophagy in which it tags damaged mitochondria with ubiquitin to signal removal via the autophagosome. Therefore, we initially wanted to use Parkin translocation in HeLa cells to confirm mitophagy induction, however it became evident that CCCP treatment of Parkin transfected cells resulted in nuclear condensation and cell death as early as 6 hours (Figure 3.10A). Therefore, we instead confirmed CCCP-induced mitochondrial depolarization using Mitrotracker CMXRos in the absence of ectopic Parkin

expression. MitoTracker CMXRos is a lipophilic cationic fluorescent dye that concentrates inside the mitochondrial matrix, via attraction to the negative membrane potential of polarized mitochondria. Upon depolarization however, a decrease in membrane potential results in less accumulation of the dye, and therefore less fluorescent emission (Pendergrass, Wolf & Poot, 2004). In doing this we confirmed that membrane potential is sufficiently reduced after 24 hours of 10 µM CCCP application (Figure 3.10B).

Using these parameters we transfected HeLa cells with a plasmid expressing Tp53INP2-mcherry and subjected these cells to 24 hours of CCCP treatment. As depicted in Figure 3.11, prior to mitochondrial stress induction Tp53INP2 is localized to the nucleus. However, upon treatment with CCCP Tp53INP2 shuttles out of the nucleus, forming punctae structures in the cytosol. Additionally, when Tp53INP2 is co-transfected with the key autophagosomal protein LC3, the application of mitochondrial stress not only causes Tp53INP2 to translocate out of the nucleus but causes it to co-localize with LC3 punctae in the cytosol (Figure 3.12). This result provides indication that Tp53INP2 not only responds to CCCP-induced mitochondrial stress by undergoing nucleocytoplasmic shuttling, but its co-localization with LC3 suggests its possible role in mitophagy.

A

B
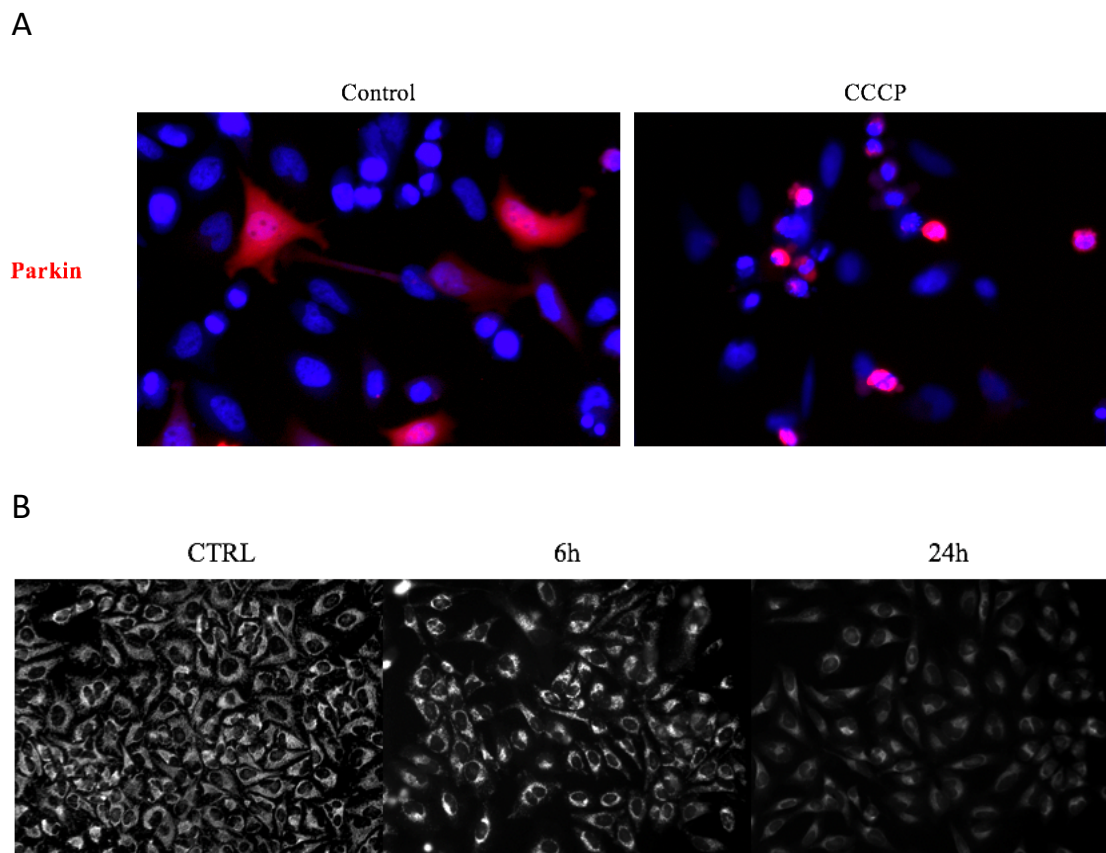
Figure 3.10. CCCP treatment of HeLa cells results in mitochondrial depolarization. To determine whether CCCP treatment results in Parkin translocation to the mitochondria, we transfected HeLa cells with a Parkin-mCherry expressing plasmid (red). Prior to CCCP-induced mitochondrial stress, Parkin is distributed diffusely within the cell (left). Upon 24 hours of CCCP treatment, Parkin transfected cells display nuclear condensation and apoptotic morphology (right). *B*. HeLa cells treated with CCCP for 6 or 24 hours and stained with MitoTracker CMXRos display reduced fluorescence than the control.
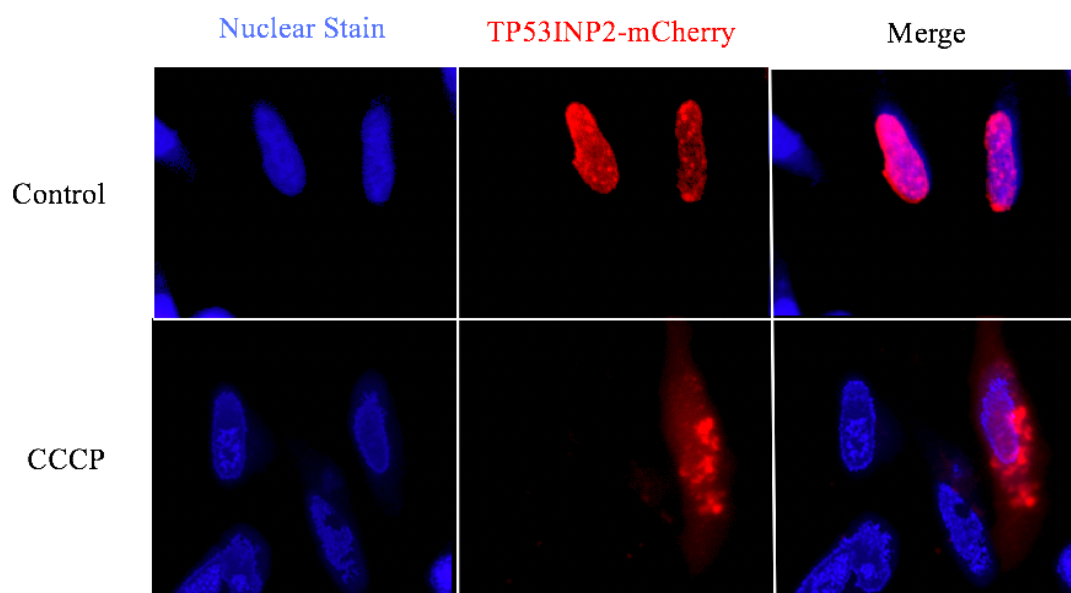
Figure 3.11. CCCP treatment induces Tp53INP2 nucleocytoplasmic shuttling in HeLa cells. Cells were transfected with Tp52INP2-mcherry then treated with 10 µM CCCP for 24 hours (second row) or left untreated (first row). Cells were fixed and stained with Hoechst nuclear stain (blue). In unstressed cells TP53INP2 is confined to the nucleus as demonstrated in the merged image. Upon CCCP treatment for 24 hours TP53INP2 shuttles out of the nucleus forming punctate structures in the cytosol.
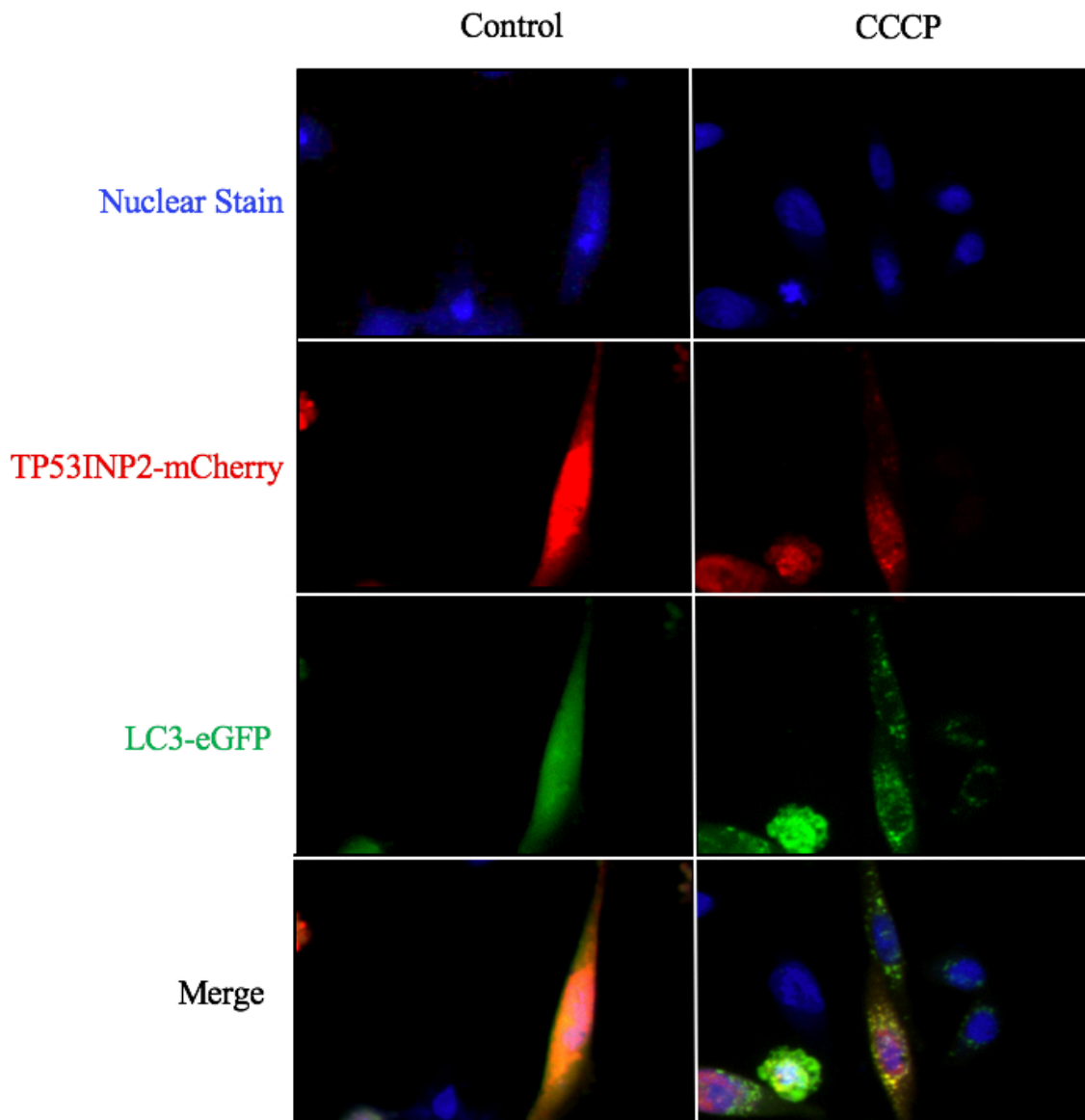
Figure 3.12. CCCP treatment induces co-localization of Tp53INP2 and LC3 in HeLa cells. Cells were co-transfected with Tp53INP2-mcherry and LC3-eGFP. The first column shows untreated cells expressing Tp53INP-mcherry in its characteristic nuclear distribution and LC3-eGFP expressed diffusely within the cell. However, upon 24 hours CCCP (10 μM) treatment, Tp53INP2 relocates from the nucleus to the cytosol. Additionally, LC3-eGFP forms punctate structures within the cytosol characteristic of autophagosomes. In the last row, the merged image demonstrates that upon CCCP mitophagy induction, Tp53INP2-mcherry co-localizes with LC3-eGFP, as indicated by the yellow fluorescence.

3.7   Ectopic expression of Tp53INP2 does not sensitize HeLa cells to mitophagy induction.

Previously a study investigating the role of Tp53INP1 and Tp53INP2 as dual regulators of autophagy demonstrated that ectopic expression of either gene in HeLa cells in the presence of lysosomal inhibitor Baf A1, resulted in increased LC3-II levels during nutrient deprivation in comparison to the controls (Sancho, et al., 2012). To determine if Tp53INP2 overexpression sensitizes cells to mitophagy induction we transfected HeLa cells with Tp53INP2 and subjected them to 24 hours of $10\mu M$ CCCP. Furthermore, we too included Baf A1 to prevent autophagosomal turnover and assess autophagic flux. As shown in Figure 3.13, western blot analysis demonstrates that ectopic expression of Tp53INP2 during CCCP-induced mitochondrial stress, resulted in increased mitophagy as measured by changes in LC3-II levels. However, although there is a trend towards Tp53INP2 expression increasing the level of CCCP-induced LC3-II formation, it did not reach statistical significance. Additionally, these changes are recapitulated with the addition of Baf A1, in which Tp53INP2 overexpression does not result in enhanced mitophagy.

In summary we demonstrated that Tp53INP2 responds to CCCP-induced mitochondrial stress induction by shuttling out of the nucleus and colocalizing with autophagosomal protein LC3, however ectopic expression of Tp53INP2 does not sensitize the cells to CCCP-induced mitophagy.

A
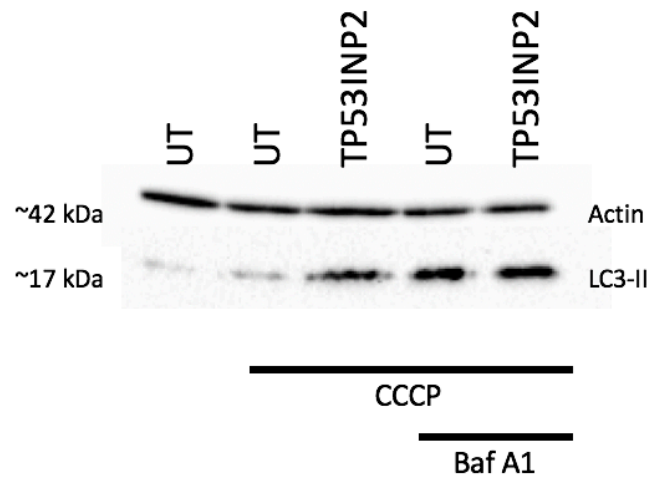
B
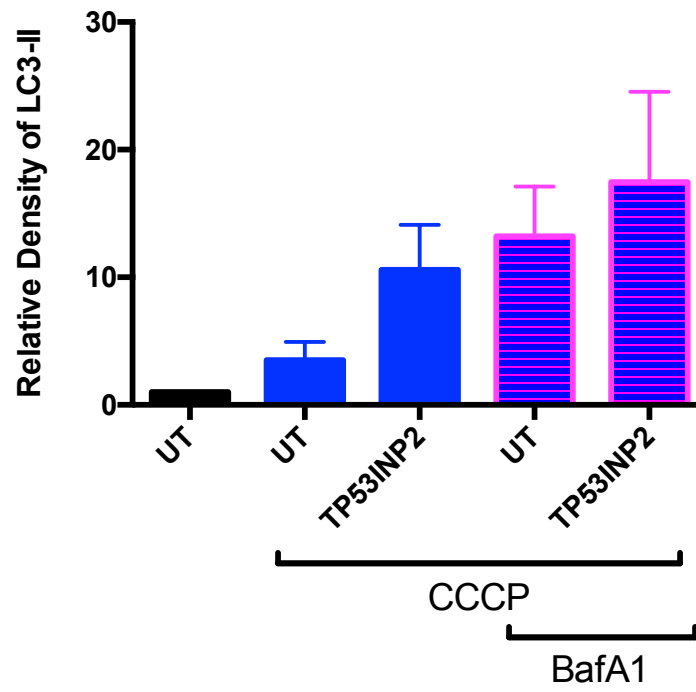
Figure 3.13. Ectopic expression of Tp53INP2 does not sensitizes HeLa cells to CCCP-induced mitophagy. HeLa cells were transfected with TP53INP2 and subjected to mitochondrial stress with treatment of 10μM CCCP for 24 hours. *A.* Western blot analysis of LC3-II levels in HeLa cells transfected with TP53INP2 and treated with 10 μM CCCP and 100 nM bafilomycin A1 (Baf A1). *B.* Graphical representation of mitophagy measured with LC3-II levels normalized to Actin. Cells transfected with Tp53INP2 demonstrate greater mitophagy in comparison to untransfected (UT) controls. Relative density was quantified using ImageLab. Data is shown as mean ± SEM of 3 independent experiments.

Chapter 4

4   Discussion

Autophagy is highly conserved cellular process that function in ensuring the turnover of proteins and organelles in a number of different cell types. The process plays a particular importance in highly specialized neurons, in which the integrity of the structure and function is sensitive to defects in autophagy. Unlike other cell types the unique, post-mitotic nature of neuronal cells necessitates a need for turnover of cellular contents to prevent the accumulation of aberrant proteins and organelles that would normally become diluted through cellular division. Previous autophagy-related gene loss of function studies have demonstrated the importance of autophagy in the central nervous system and how its dysregulation can contribute to the formation of protein aggregates and neurodegeneration (Komatsu, et al., 2006). Neuronal autophagy plays a vital role in maintaining neuronal metabolic and nutrient homeostasis, preventing the accumulation of toxic proteins and damaged organelles. Defects in autophagy have been notable in various neurodegenerative diseases including, Parkinson's disease, Alzheimer's disease and Huntington's disease (Nixon & Yang, 2012). Previously studies had investigated the role of Tp53INP1in non-neuronal autophagy using mammalian cell lines to demonstrate that cells deficient in Tp53INP1 demonstrated impaired autophagy and higher sensitivity to stress-induced cell death. It has also been observed that mouse embryonic fibroblast cells (MEFs) deficient in Tp53INP1 display less effective mitophagy leading to the accumulation of damaged mitochondria and increased ROS production. Therefore, the goal of this work was to determine whether Tp53INP1 plays an important role in neuronal autophagy. Our results have demonstrated that Tp53INP1 plays a role in neuronal autophagy as its absence results in attenuated autophagy induction in response to trophic factor deprivation and hypoxic stress in both cerebellar granule neurons and primary cortical neuron, respectively. We've also demonstrated that Tp53INP2 responds to mitochondrial stress induction, however its expression does not sensitize cells to mitophagy induction.

4.1   Tp53INP1 plays a role in neuronal autophagy

The main aim of this study was to determine if Tp53INP1 plays a role in neuronal autophagy and mitophagy. Previously studies using human bone osteosarcoma cells (U2OS) and MEFs demonstrated that Tp53INP1 participated in autophagy (Seillier , et al., 2012) and mitophagy (Seillier, et al., 2015), respectively. These studies demonstrated that Tp53INP1 interacts with autophagy-related proteins upon nutrient deprivation and rapamycin by colocalizing with LC3 in the cytosol. This study also demonstrated that once localized to the autophagosome, Tp53INP1 is degraded by autophagy, much like other autophagosome related proteins (Seillier, et al., 2012). This same group also established that MEFs deficient in Tp53INP1 displayed an accumulation of defective mitochondria resulting from impaired mitophagy (Seillier, et al., 2015). To determine if Tp53INP1 plays an important role to neuronal autophagy, we used two paradigms of established neuronal autophagy induction, and compared the effect of the presence and absence of Tp53INP1 on the induction of autophagy.

4.1.1   Tp53INP1-deficient CGNs display attenuated trophic deprivation-induced autophagy

Cerebellar granule neurons (CGNs) are a widely employed model for the investigation of neuronal apoptosis, and the role of autophagy in cell death is becoming more and more apparent (Canu, et al., 2005). CGNs cultured in medium containing 25 mM KCl (K25) and transferred to media containing 5 mM KCl (K5) undergo trophic factor deprivation-induced apoptosis, displaying apoptotic features after 24 hours (Maycotte, Guemez-gamboa, & Moran, 2010). Additionally, previous studies have demonstrated the formation of autophagosomes preceding apoptotic induction via potassium deprivation, therefore we investigated whether Tp53INP1 plays a role in neuronal autophagy using a trophic factor deprivation paradigm in CGNs.

In order to capture autophagic flux the use of autophagosomal inhibitors such as Baf A1 and CQ are necessary. For this reason, we began by determining the kinetics of

autophagosome formation by comparing the effects of both inhibitors to determine the kinetics of trophic deprivation on CGNs extracted from CD1 mice. We observed that K5 treatment for 12 hours resulted in a significant reduction in cell survival, which occurred earlier than described in previous reports (Maycotte, Guemez-gamboa, & Moran, 2010). This may be attributed to differences in paradigms in which our study elicited the use the lysosomal inhibitor chloroquine, an agent that causes the inhibition of autophagy by preventing autophagosome turnover. Interestingly, previous studies had found that the inhibition of autophagy with 3-MA protected CGNs from K5-induced cell death (Maycotte, Guemez-gamboa, & Moran, 2010). However, this is likely ascribed to the difference in inhibitory action of the above inhibitors; 3-MA prevents the initiation of autophagy by inhibiting the class III PI3K Vsp34, which serves to regulate autophagosome biogenesis through the production of phosphoinositides (Fougeray and Pallet, 2014). CQ however, is a lysomotrophic compound that prevents acidification of the lysosome, thereby inhibiting fusion between the autophagosome and the lysosome. This blockage in late stage autophagy results in an accumulation of autophagosomes which can induce toxicity and death (Button et al., 2017).

We then subjected CGNs extracted from CD1 mice (P7) to K5 potassium deprivation for up to 6 hours and observed significant increases in autophagic flux at 4 and 6 hours. When we subjected CGNs extracted from Tp53INP1 transgenic mice to the same conditions, we observed a significant reduction in the level of autophagy at 6 hours in the Tp53INP1 – deficient neurons compared to the wildtype littermates. Additionally, we conducted immunofluorescence (IF) staining of LC3, and observed significantly less LC3 in the Tp53INP1$^{-/-}$ CGNs at 2 and 4 hours of K5 conditions as well as in the control. Interestingly this finding suggests that not only is stress-induced autophagy impaired in absence of Tp53INP1, but basal autophagy may be as well. Furthermore, it would be interesting to see if this reduction in autophagy protects Tp53INP1-deficient neurons from autophagic cell death, as has been observed when inhibiting autophagy with 3-MA (Canu, et al., 2005).

4.1.2 Tp53INP1- deficient PCNs display attenuated hypoxia-induced autophagy

In order to further investigate the role of Tp53INP1 in neuronal autophagy, we used an hypoxia/ischemia paradigm in primary cortical neurons (PCNs), as oxygen-deprivation is one of the most established inducers of autophagy (Fang et al., 2015). Several studies have demonstrated that autophagy is rapidly activated in neurons exposed to hypoxic-ischemic conditions (Carloni, Buonocore, and Balduini, 2008; Zhu, et al., 2004) however whether the cell induces autophagy to clear itself of damaged organelles and toxic metabolites in efforts to promote survival, or whether it promotes cell death through excessive self-digestions is still in question. For this reason, there is currently no unified theory on whether autophagy plays a neuroprotective role or contributes to neurodegeneration under these conditions.

Autophagic responses to hypoxia are said the be regulated differently depending on the severity of the insult, as well as the maturity of the brain (Gabryel, Kost and Kasprowska, 2012). In chronic and moderate hypoxic conditions autophagy is regulated by hypoxia-inducible factor 1α (HIF-1α), a transcription factor that allows adaption to a large range of oxygen concentrations (Mazure & Pouyssegur, 2010). In acute and severe hypoxic conditions however, autophagy is regulated by HIF-1α-independent pathways, such as mTOR (Mazure & Pouyssegur, 2010). The differential response of neurons to hypoxic environments have been demonstrated by several studies that provide evidence for both neuroprotective and cell death pathways of autophagy. For example neonatal mice subjected to hypoxic/ischemic (HI) injury demonstrate increased autophagosome formation and dramatic hippocampal neuronal death (Koike & Shibata, 2008) whereas contradictory studies demonstrate that increasing autophagy via rapamycin in neonatal rats subjected to HI demonstrated a reduction in necrotic cell death as well as decreased brain injury (Carloni, Buonocore and Balduini, 2008). Therefore, greater understanding of the autophagy during HI is necessary to better grasp its potential role in stroke afflicted brains.

In the present study we used a hypoxic stress paradigm to begin determining whether Tp53INP1 functions in neuronal autophagy. We initially used PCNs from non-transgenic CD1 mice to determine the effect of hypoxia on neuronal autophagy. We also treated the

neurons with the CQ to capture autophagic flux; the complete process of autophagy from cargo sequestration to delivery and degradation by the lysosome (Klionsky, et al., 2009). In the absence of the agent, the cells exhibit rapid autophagic turnover (Appendix C), which necessitates its use in our experiments.

These CD1 neurons demonstrated increases in autophagic flux with increased exposure to hypoxic environments for up to 8 hours as measured by the conversion of LC3-I to LC3-II (Figure 3.6). This is in alignment with several studies indicating increases in autophagy induction after hypoxia-ischemic exposure (Bellot, et al., 2009; Mazure and Pouysségur, 2010; Naves et al., 2013). We had originally found that PCN from CD1 mice demonstrate steady increases in autophagy for up to 24 hours of hypoxia, but opted on using shorter time frames as 1) we saw robust increases of LC3-II at earlier durations, and 2) we did not know the extent of the effect of Tp53INP1 deficiency in neuronal autophagy, and therefore opted to avoid the possibility of high levels of apoptosis affecting our cultures. Using these parameters, we subjected PCNs from transgenic Tp53INP1 mice to the same hypoxic conditions and found that PCNs from Tp53INP1$^{-/-}$ mice displayed significantly less increases in autophagy in response to increased duration of hypoxia, specifically at 4 and 8 hours of exposure, than we had observed for their wild type littermates. In support of this, when we conducted IF and stained for LC3, we observed less LC3 staining after 8 hours of hypoxic exposure in the Tp53INP1$^{-/-}$ neurons compared to the wild types (Figure 3.8). This result suggests that Tp53INP1-deficient PCNs, have reduced autophagic responses to hypoxic stress.

Another method of autolysosome detection uses an acidotrophic dye called monodansylcadaverine (MDC), which accumulates in the acidic vacuoles such as lysosomes and autolysosomes of PCNs (Maycotte, Guemez-gamboa, & Moran, 2010). An increase from basal lysosomal staining upon autophagy induction would be indictive of increased autolysosome formation (Niemann, Takatsuki & Elsässer, 2000). We would expect to see an increase in MDC staining in Tp53INP1-present cells and very little change from basal lysosome staining in the Tp53INP1-deficient PCNs.

In addition to this the level of p62, a protein that binds to LC3 of the inner autophagosomal membrane as well as ubiquitin residues of the cargo, can be measured. In the absence of lysosomal inhibitors, p62 accumulation should inversely correlate to the level of autophagy

(Petibone, Majeed, & Casciano, 2016). Furthermore, we are currently developing Adenoviral vectors expressing Tp53INP1, of which can serve to reintroduce the gene into Tp53INP1-deficient PCNs to determine if this rescues the reduced autophagy observed in these experiments. Additionally, it would be interesting to investigate into the ongoing debate of whether increased autophagy enhances cell survival during hypoxic stress or induces cell death. This can be investigated by determining whether this reduction in autophagy induction in Tp53INP1$^{-/-}$ PCNs sensitizes the neurons to hypoxia-induced cell death, or whether it confers an increased resistance to apoptosis. This can be explored using a caspase assay to measure the number of apoptotic cells by detecting the increase in fluorescence with the conversion of the caspase-3 substrate DEVD-AMC into AMC (Poreba, Strozyk, Salvesen & Drag, 2013). Moreover, to evaluate whether autophagy and apoptosis are taking place at the same time, we can perform IF staining of LC3 in combination with TUNEL staining to determine if cells exhibit both markers for autophagy and apoptosis, respectively (Maycotte, Guemez-gamboa, & Moran, 2010).

4.2 Ischemic injury/reperfusion increase autophagic flux in PCNs

Cerebral ischemia (ischemic stroke) arises from the lack of blood supply and therefore oxygen and nutrients to a localized area of the brain, resulting from blockage of blood vessels via a thrombus or embolus (Kalogeris, Baines , Krenz , & Korthuis, 2012). This results in damage that typically occurs within 1-2 minutes, and results in profound reductions in ATP levels and extensive cell death, specifically in the region immediately affected called the core (Tang, Tian , Yi , & Chen , 2016). The current therapeutic approach is called reperfusion, the restoring of blood flow to the brain through administration of anticoagulant drugs, such as alteplase and aspirin (Tang, Tian , Yi , & Chen , 2016). Reperfusion however poses dangers as the rapid reintroduction of oxygen often results in the formation of oxygen radicals which results in further damage through the signaling of proinflammatory responses (de Vries et al., 2013). Previous studies have demonstrated increased autophagy induction upon ischemic/reperfusion paradigms and have contributed conflicting results upon how autophagic inductions affects ischemic damage. In 2006, Khan and colleagues demonstrated that mice pretreated with rapamycin, demonstrated

reduced infarct size in an intact heart upon ischemic insult (Khan, et al., 2006). However other studies have found that autophagy attenuation reduced cell death in cardiomyocyte ischemic/reperfusion injury (Valentim, et al., 2006). Therefore, understanding the role of autophagy in cerebral ischemia and injury could contribute to improved therapeutic approach.

We modelled ischemia by subjecting PCNs extracted from CD1 mice to 2 hours incubation in an OGD media and hypoxic environment. After the 2 hours of ischemic insult, the neurons underwent reperfusion (RP) through incubation in glucose-containing media and normoxic conditions for up to 12 hours. Since OGD (ischemia) results in the lack of nutrients, there is no surprise that autophagy is rapidly induced, however the question remains whether this increase also results in increased neuronal cell death. This initial experiment served to identify the appropriate parameters to elicit ischemic insults on PCN cultured from Tp53INP1 transgenic mice, however we were unable to pursue this at the time due to insufficient number of neurons.

Lastly, these hypoxia/ischemia paradigms would serve as an excellent model to investigate the role of Tp53INP1 in neuronal mitophagy. It was previously demonstrated that Tp53INP1 knockout MEFs had increased expression of BNIP3 and NIX, suggesting that hypoxia-induced mitophagy was not affected by Tp53INP1 deficiency (Seillier, et al., 2015). However, our studies in PCNs exposed to hypoxic stress suggests that autophagy and possibly mitophagy may be affected. It would be interesting to compare the protein levels of BNIP3 and NIX in Tp53INP1 wild-type and knockout cells. If Tp53INP1 does in fact play a large role in neuronal mitophagy, as an increase in these mitophagy proteins in the absence of Tp53INP1 could also suggest the cells ability to compensate and still undergo hypoxia-induced mitophagy.

4.3   Tp53INP2 responds to mitochondrial stress

In previous studies, it was demonstrated that Tp53INP2 participates in mTOR-dependent mammalian autophagy, and this function is attributed to its ability to shuttle out of the nucleus to the cytosol where it could interact with autophagy-related proteins (Mauvezin et al., 2012; Nowak et al., 2009b). Many of these studies were primarily conducted in HeLa cells, therefore we utilized these cells to investigate if Tp53INP2 responds to mitochondrial

stress induction, which had not been demonstrated to our knowledge in either non-neuronal nor neuronal cells. We used the ionophore CCCP to dissipate the mitochondrial proton gradient, an event that according to previous literature is sufficient to induce mitophagy (Sargsyan et al., 2015; Wang, Nartiss, Steipe, McQuibban, & Kim, 2012). We transfected HeLa cells with Tp53INP2-mCherry and subjected them to 24 hours of 10 μM CCCP treatment. In doing this we observed that CCCP treatment resulted in Tp53INP2 undergoing nucleocytoplasmic shuttling, forming punctae in the cytosol (Figure 3.11). This result demonstrated that Tp53INP2 responds to mitochondrial stress. However, whether or not its response was due to mitophagy induction was still unknown. Previously multiple studies had demonstrated that the colocalization of Tp53INP2 to LC3 was indicative that the protein likely plays a role in an autophagic response, although not confirmation of its interaction with the autophagosome (Nowak, et al., 2012; Sancho, et al., 2012). Therefore, we cotransfected HeLa cells with both LC3-eGFP and Tp53INP2-mCherry and subjected the cells to 24 hours of 10 μM CCCP. In doing this we observed that Tp53INP2-mCherry not only shuttled out of the nucleus into the cytosol, but also colocalized with newly formed LC3 puncta as indicated by the yellow fluorescence (Figure 3.12). This result gave us the first lead indicating that Tp53INP2, like its homolog Tp53INP1 (Seillier, et al., 2015) may play a role in mitophagy. To further confirm this finding and determine if Tp53INP2 and LC3 also colocalize with the mitochondria, we could immunostain for mitochondrial protein TOM20. The colocalization of all three markers provide further support that Tp53INP2 does in fact participate in mitophagy.

In order to determine whether Tp53INP2 is necessary for mammalian mitophagy, future studies could investigate if the loss of Tp53INP2 attenuates mitophagy. To do this we could elicit the use of the CRISPR/Cas9 gene editing tool to generate a TP53INP2- deficient HeLa cell line (Sun, Lutz, & Tao, 2016). The level of mitophagy could be measured by comparing the number of LC3-positive punctae per cell, with and without CCCP treatment, in Tp53INP2 present and deficient HeLa cells. If Tp53INP2 is a necessary player in mammalian mitophagy, we expect this number to decrease, indicating attenuated mitophagy in response to the same mitochondrial stressor. In addition to this we would expect a decrease in the LC3-II/LC3-I ratio through western blot analysis in Tp53INP2-deficient cells in response to mitophagy inducers. To further support this idea, we could

reintroduce Tp53INP2 into Tp53INP2-deficient HeLa cells and determine if reintroduction results in an increase in LC3 punctae, thereby rescuing mitophagy induction.

4.4 Ectopic expression of Tp53INP2 does not sensitize HeLa cells to mitophagy induction

Although the shuttling of Tp53INP2 in response to mitochondrial depolarization suggested that Tp53INP2 may participate in mitophagy, previous studies had demonstrated that the overexpression of Tp53INP2 in HeLa enhances autophagic flux during starvation compared to a pcDNA control as measured by changes in LC3-II levels (Sancho, et al., 2012; Mauvezin, et al., 2010). Therefore, we aimed to determine if overexpression of Tp53INP2 sensitizes cells to mitophagic induction in response to mitochondrial depolarization. We transfected HeLa cells and used the same parameters as our previous paradigm, subjecting the cells to 24 hours of 10 µM CCCP treatment. When Tp53INP2-transfected cells are subjected to CCCP-induced mitochondrial stress, the cells do not display levels of mitophagy significantly greater than that of the control. Additionally, in the presence of Baf A1, we observed higher levels of LC3-II in both UT and Tp53INP2-transfected, however similar to the CCCP alone group, we observed no significant differences between the two.

Although ectopic expression of Tp53INP2 does not sensitize cells to mitophagic induction, it does not negate the fact that the protein undergoes nucleocytoplasmic shuttling in response to mitochondrial depolarization. Therefore, Tp53INP2 may not enhance mitophagy, but instead play a role in facilitating it.

Chapter 5

5 Conclusion

Autophagy has been found to play vital roles in both basal neuronal homeostasis and under stress conditions such as hypoxic/ischemic insult. Previous studies have demonstrated the role of nuclear proteins Tp53INP1 and Tp53INP2 in mammalian autophagy. In this study. we demonstrated that in the absence of Tp53INP1, neuronal autophagy induced via hypoxia and trophic factor deprivation is attenuated. We also demonstrated that Tp53INP2 responds to mitochondrial stress by shuttling out of the nucleus and colocalizing with autophagosomal marker LC3. These results suggest a functional role of Tp53INP1 in neuronal autophagy and provides a possible target for autophagy regulation in neuronal injury paradigms.

References

Ashrafi, G. and Schwarz, T. (2012). The pathways of mitophagy for quality control and clearance of mitochondria. *Cell Death & Differentiation*, 20(1), pp.31-42.

Balázs, R., Gallo, V. and Kingsbury, A. (1988). Effect of depolarization on the maturation of cerebellar granule cells in culture. *Developmental Brain Research*, 40(2), pp.269-276.

Bellot, G., Garcia-Medina, R., Gounon, P., Chiche, J., Roux, D., Pouyssegur, J. and Mazure, N. (2009). Hypoxia-Induced Autophagy Is Mediated through Hypoxia-Inducible Factor Induction of BNIP3 and BNIP3L via Their BH3 Domains. *Molecular and Cellular Biology*, 29(10), pp.2570-2581.

Button, R., Roberts, S., Willis, T., Hanemann, C. and Luo, S. (2017). Accumulation of autophagosomes confers cytotoxicity. *Journal of Biological Chemistry*, 292(33), pp.13599-13614.

Canu, N., Tufi, R., Serafino, A., Amadoro, G., Ciotti, M. and Calissano, P. (2005). Role of the autophagic-lysosomal system on low potassium-induced apoptosis in cultured cerebellar granule cells. *Journal of Neurochemistry*, 92(5), pp.1228-1242.

Carloni, S., Buonocore, G. and Balduini, W. (2008). Protective role of autophagy in neonatal hypoxia–ischemia induced brain injury. *Neurobiology of Disease*, 32(3), pp.329-339.

de Vries, D., Kortekaas, K., Tsikas, D., Wijermars, L., van Noorden, C., Suchy, M., Cobbaert, C., Klautz, R., Schaapherder, A. and Lindeman, J. (2013). Oxidative Damage in Clinical Ischemia/Reperfusion Injury: A Reappraisal. *Antioxidants & Redox Signaling*, 19(6), pp.535-545.

Filadi, R., Pendin, D. and Pizzo, P. (2018). Mitofusin 2: from functions to disease. *Cell Death & Disease*, 9(3).

Fougeray, S. and Pallet, N. (2014). Mechanisms and biological functions of autophagy in diseased and ageing kidneys. *Nature Reviews Nephrology*, 11(1), pp.34-45.

Gabryel, B., Kost, A. and Kasprowska, D. (2012). Neuronal autophagy in cerebral ischemia – a potential target for neuroprotective strategies?. *Pharmacological Reports*, 64(1), pp.1-15.

Gommeaux, J., Cano, C., Garcia, S., Gironella, M., Pietri, S., Culcasi, M., Pébusque, M., Malissen, B., Dusetti, N., Iovanna, J. and Carrier, A. (2007). Colitis and Colitis-Associated Cancer Are Exacerbated in Mice Deficient for Tumor Protein 53-Induced Nuclear Protein 1. *Molecular and Cellular Biology*, 27(6), pp.2215-2228.

Liu, K., Sun, X., Chen, W. and Sun, Y. (2014). Autophagy: a double-edged sword for neuronal survival after cerebral ischemia. *Neural Regeneration Research*, 9(12), p.1210.

Mazure, N. and Pouysségur, J. (2010). Hypoxia-induced autophagy: cell death or cell survival?. *Current Opinion in Cell Biology*, 22(2), pp.177-180.

Naves, T., Jawhari, S., Jauberteau, M., Ratinaud, M. and Verdier, M. (2013). Autophagy takes place in mutated p53 neuroblastoma cells in response to hypoxia mimetic CoCl2. *Biochemical Pharmacology*, 85(8), pp.1153-1161.

Nedelsky, N., Todd, P., & Taylor, J. (2008). Autophagy and the ubiquitin-proteasome system: Collaborators in neuroprotection. *Biochimica Et Biophysica Acta (BBA) - Molecular Basis Of Disease*, *1782*(12), 691-699. doi: 10.1016/j.bbadis.2008.10.002

Niemann, A., Takatsuki, A., & Elsässer, H. (2000). The Lysosomotropic Agent Monodansylcadaverine Also Acts as a Solvent Polarity Probe. *Journal Of Histochemistry & Cytochemistry*, *48*(2), 251-258. doi: 10.1177/002215540004800210

Nixon, R., & Yang, D. (2012). Autophagy and Neuronal Cell Death in Neurological Disorders. *Cold Spring Harbor Perspectives In Biology*, *4*(10), a008839-a008839. doi: 10.1101/cshperspect.a008839

Nowak, J., Archange, C., Tardivel-Lacombe, J., Pontarotti, P., Pébusque, M., & Vaccaro, M. et al. (2009). The TP53INP2 Protein Is Required for Autophagy in Mammalian Cells. *Molecular Biology Of The Cell*, *20*(3), 870-881. doi: 10.1091/mbc.e08-07-0671

Pendergrass, W., Wolf, N., & Poot, M. (2004). Efficacy of MitoTracker Green? and CMXrosamine to measure changes in mitochondrial membrane potentials in living cells and tissues. *Cytometry*, *61A*(2), 162-169. doi: 10.1002/cyto.a.20033

Petibone, D., Majeed, W., & Casciano, D. (2016). Autophagy function and its relationship to pathology, clinical applications, drug metabolism and toxicity. *Journal Of Applied Toxicology*, *37*(1), 23-37. doi: 10.1002/jat.3393

Redmann, M., Benavides, G., Berryhill, T., Wani, W., Ouyang, X., & Johnson, M. et al. (2017). Inhibition of autophagy with bafilomycin and chloroquine decreases mitochondrial quality and bioenergetic function in primary neurons. *Redox Biology*, *11*, 73-81. doi: 10.1016/j.redox.2016.11.004

Redmann, M., Dodson, M., Boyer-Guittaut, M., Darley-Usmar, V., & Zhang, J. (2014). Mitophagy mechanisms and role in human diseases. *The International Journal Of Biochemistry & Cell Biology*, *53*, 127-133. doi: 10.1016/j.biocel.2014.05.010

Rui, Y., Xu, Z., Patel, B., Chen, Z., Chen, D., & Tito, A. et al. (2015). Huntingtin functions as a scaffold for selective macroautophagy. *Nature Cell Biology*, *17*(3), 262-275. doi: 10.1038/ncb3101

Saadi, H., Seillier, M., & Carrier, A. (2015). The stress protein TP53INP1 plays a tumor suppressive role by regulating metabolic homeostasis. *Biochimie*, *118*, 44-50. doi: 10.1016/j.biochi.2015.07.024

Sancho, A., Duran, J., García-España, A., Mauvezin, C., Alemu, E., & Lamark, T. et al. (2012). DOR/Tp53inp2 and Tp53inp1 Constitute a Metazoan Gene Family Encoding Dual Regulators of Autophagy and Transcription. *Plos ONE*, *7*(3), e34034. doi: 10.1371/journal.pone.0034034

Seillier, M., Peuget, S., Gayet, O., Gauthier, C., N'Guessan, P., & Monte, M. et al. (2012). TP53INP1, a tumor suppressor, interacts with LC3 and ATG8-family proteins through the LC3-interacting region (LIR) and promotes autophagy-dependent cell death. *Cell Death & Differentiation*, *19*(9), 1525-1535. doi: 10.1038/cdd.2012.30

Son, J., Shim, J., Kim, K., Ha, J., & Han, J. (2012). Neuronal autophagy and neurodegenerative diseases. *Experimental & Molecular Medicine*, *44*(2), 89. doi: 10.3858/emm.2012.44.2.031

Song, M., Mihara, K., Chen, Y., Scorrano, L., & Dorn, G. (2015). Mitochondrial Fission and Fusion Factors Reciprocally Orchestrate Mitophagic Culling in Mouse Hearts and Cultured Fibroblasts. *Cell Metabolism*, *21*(2), 273-286. doi: 10.1016/j.cmet.2014.12.011

Stolz, A., Ernst, A., & Dikic, I. (2014). Cargo recognition and trafficking in selective autophagy. *Nature Cell Biology*, *16*(6), 495-501. doi: 10.1038/ncb2979

Sun, L., Lutz, B. M., & Tao, Y.-X. (2016). The CRISPR/Cas9 system for gene editing and its potential application in pain research. Translational Perioperative and Pain Medicine , 1(3), pp.22-33.

Tang, Y., Tian, H., Yi, T., & Chen, H. (2016). The critical roles of mitophagy in cerebral ischemia. *Protein & Cell*, *7*(10), 699-713. doi: 10.1007/s13238-016-0307-0

Tanida, I., Ueno, T., & Kominami, E. (2004). LC3 conjugation system in mammalian autophagy. *The International Journal Of Biochemistry & Cell Biology*, *36*(12), 2503-2518. doi: 10.1016/j.biocel.2004.05.009

Valentim, L., Laurence, K., Townsend, P., Carroll, C., Soond, S., & Scarabelli, T. et al. (2006). Urocortin inhibits Beclin1-mediated autophagic cell death in cardiac myocytes exposed to ischaemia/reperfusion injury. *Journal Of Molecular And Cellular Cardiology*, *40*(6), 846-852. doi: 10.1016/j.yjmcc.2006.03.428

Villa, E., Proïcs, E., Rubio-Patiño, C., Obba, S., Zunino, B., & Bossowski, J. et al. (2017). Parkin-Independent Mitophagy Controls Chemotherapeutic Response in Cancer Cells. *Cell Reports*, *20*(12), 2846-2859. doi: 10.1016/j.celrep.2017.08.087

Wang, Y., Nartiss, Y., Steipe, B., McQuibban, G., & Kim, P. (2012). ROS-induced mitochondrial depolarization initiates PARK2/PARKIN-dependent mitochondrial degradation by autophagy. *Autophagy*, *8*(10), 1462-1476. doi: 10.4161/auto.21211

Wen, Y.-D., Sheng, R., Zhang, L.-S., Han, R., Zhang , X., Zhang , X.-D., . . . Qin, Z.-H. (2008). Neuronal injury in rat model of permanent focal cerebral ischemia is associated with activation of autophagic and lysosomal pathways. Autophagy, 4(6), pp.762-769.

Zhang, X., Yan, H., Yuan, Y., Gao, J., Shen, Z., & Cheng, Y. et al. (2013). Cerebral ischemia-reperfusion-induced autophagy protects against neuronal injury by mitochondrial clearance. *Autophagy*, *9*(9), 1321-1333. doi: 10.4161/auto.25132

Zhu, C., Wang, X., Xu, F., Bahr, B., Shibata, M., & Uchiyama, Y. et al. (2004). The influence of age on apoptotic and other mechanisms of cell death after cerebral hypoxia–ischemia. *Cell Death And Differentiation*, *12*(2), 162-176. doi: 10.1038/sj.cdd.4401545

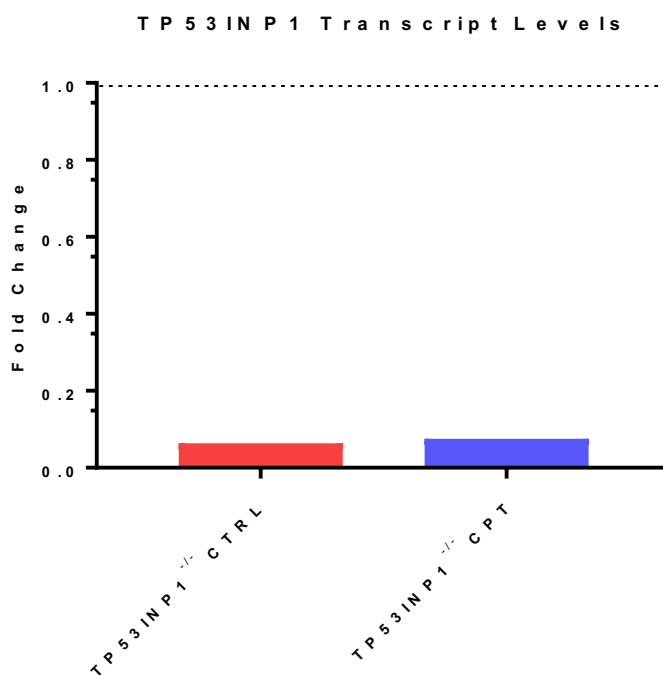# Appendices

Appendix A: TP53INP1 Knock-out genotyping

Figure 6.0.1. TP53INP1 mRNA transcript levels to confirm genotyping. Tp53INP1^{-/-} mice were treated with camptothecin (CPT), a naturally occurring alkaloid that inhibits DNA and RNA synthesis in mammalian cells. CPT treatment has previously been demonstrated to cause increased Tp53INP1 gene expression in primary cortical neurons of wild-type and non-transgenic mouse models in comparison to their untreated controls. However in TP53INP1^{-/-} primary cortical neurons, CPT only results in barely noticeable increase from the untreated control samples. Perhaps more importantly, the transcript levels are below 10% of that found in untreated TP53INP^{+/+} control samples, as indicated by the dashed line.
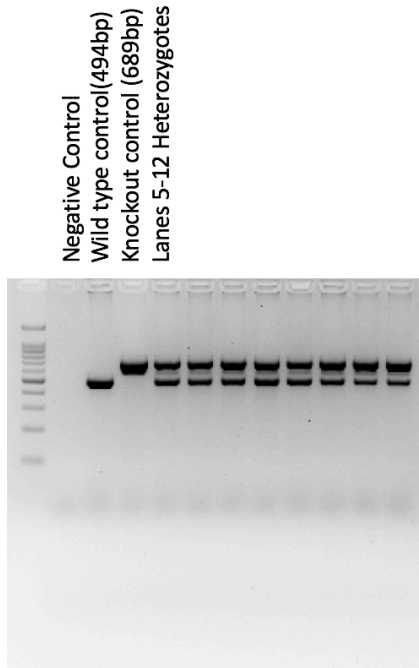
Figure 6.0.2. Genotyping agarose gel for TP53INP1 mice. The genotyping for TP53INP1 mice show wildtype bands at 494 base pairs and knockout bands at 689 base pair with both bands displayed for homozygotes. Lane 1 contains a 100 base pairs ladder from FroggaBio.

Appendix B: One-Step PCR Reagents and Cycling Conditions

Table 1: One-Step PCR Reagents and Volumes

Component	Volume (µL)	Final Concentration
2x Quanti. SYBR Green Buffer	12.5	1x
Primer A	2.5	1µM
Primer B	2.5	1µM
Quanti. RT Mix	0.25	NA
Template RNA	4	40ng/reaction
RNA free Water	3.25	NA
Total rxn volume	**25**	

Table 2: One-Step PCR Cycling Conditions

	Temperature (ºC)	Time (minutes)	Duration
1	50	10:00	x 1
2	95	5:00	x 1
3	95	0:10	x 39
4	60	0:30	
5	65	0.05	Melt Curve: 65ºC to 95ºC in 0.5ºC increments
6	95	End	

Table 3: Genotyping PCR Reagents

Reagent	Volume (µL)
10 mM dNTP's	2
10x buffer (1x)	2.5
50 mM MgCl2	1.5
Q solution	5
Qiagen Taq	0.75
Nano water	2.25
Primer #1 STINP F WT (10 µM)	3
Primer #2 STINP R WT (10 µM)	3
Primer #3 STINP R CRE (10 µM)	3
Mouse DNA sample	2
TOTAL	**25**

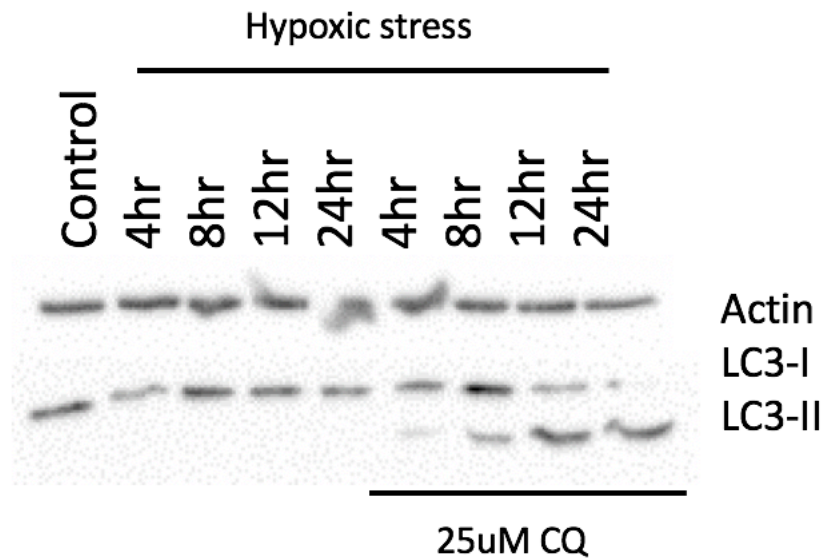# Appendix C: The effect of chloroquine on autophagic flux.

Figure 6.0.3. Autophagic flux is captured with the use of chloroquine. CD1 primary cortical neurons in which half were treated with 25 μM chloroquine, a lysosomal inhibitor and half were left untreated were subjected to hypoxic conditions of 0.5% O2 and 5% CO2 for up to 24 hours. Samples were probed for LC3-I and LC3-II, with Actin serving as a loading control. As shown, autophagic flux is only captured when the lysosomal inhibitor is included.

Curriculum Vitae

Name: Vidhyasree Shyam

Post-secondary   University of Waterloo
Education and   Waterloo, Ontario, Canada
Degrees: 2009-2015 BSc

                       Western University
                       London, Ontario, Canada
                       2016-2019 MSc

Honours and   Province of Ontario Graduate Scholarship
Awards: 2016-2017, 2017-2018

Related Work   Graduate Teaching Assistant
Experience: Western University
                       London, Ontario, Canada
                       2017-2017, 2017-2018

                       Undergraduate Teaching Assistant
                       University of Waterloo
                       Waterloo, Ontario, Canada
                       2015-2015